Dynamical susceptibility of glass formers: Contrasting the predictions of theoretical scenarios

Cristina Toninelli,[1] Matthieu Wyart,[2] Ludovic Berthier,[3] Giulio Biroli,[4] and Jean-Philippe Bouchaud[2,5]
[1]*ENS 24 rue Lhomond, 75231 Paris Cedex 05, France*
[2]*Service de Physique de l'État Condensé Orme des Merisiers—CEA Saclay, 91191 Gif sur Yvette Cedex, France.*
[3]*Laboratoire des Verres UMR 5587, Université Montpellier II and CNRS, 34095 Montpellier, France*
[4]*Service de Physique Théorique Orme des Merisiers—CEA Saclay, 91191 Gif sur Yvette Cedex, France*
[5]*Science & Finance, Capital Fund Management 6-8 Bd Haussmann, 75009 Paris, France*
(Received 15 December 2004; published 14 April 2005)

We compute analytically and numerically the four-point correlation function that characterizes nontrivial cooperative dynamics in glassy systems within several models of glasses: elastoplastic deformations, mode-coupling theory (MCT), collectively rearranging regions (CRR's), diffusing defects, and kinetically constrained models (KCM's). Some features of the four-point susceptibility $\chi_4(t)$ are expected to be universal: at short times we expect a power-law increase in time as t^4 due to ballistic motion (t^2 if the dynamics is Brownian) followed by an elastic regime (most relevant deep in the glass phase) characterized by a t or $\sqrt{t}$ growth, depending on whether phonons are propagative or diffusive. We find in both the β and early α regime that $\chi_4 \sim t^{\mu}$, where μ is directly related to the mechanism responsible for relaxation. This regime ends when a maximum of χ_4 is reached at a time $t=t^*$ of the order of the relaxation time of the system. This maximum is followed by a fast decay to zero at large times. The height of the maximum also follows a power law $\chi_4(t^*) \sim t^{*\lambda}$. The value of the exponents μ and λ allows one to distinguish between different mechanisms. For example, freely diffusing defects in $d=3$ lead to $\mu=2$ and $\lambda=1$, whereas the CRR scenario rather predicts either $\mu=1$ or a logarithmic behavior depending on the nature of the nucleation events and a logarithmic behavior of $\chi_4(t^*)$. MCT leads to $\mu=b$ and $\lambda=1/\gamma$, where b and γ are the standard MCT exponents. We compare our theoretical results with numerical simulations on a Lennard-Jones and a soft-sphere system. Within the limited time scales accessible to numerical simulations, we find that the exponent μ is rather small, $\mu<1$, with a value in reasonable agreement with the MCT predictions, but not with the prediction of simple diffusive defect models, KCM's with noncooperative defects, and CRR's. Experimental and numerical determination of $\chi_4(t)$ for longer time scales and lower temperatures would yield highly valuable information on the glass formation mechanism.

DOI: 10.1103/PhysRevE.71.041505 PACS number(s): 64.70.Pf

I. INTRODUCTION

The idea that the sharp slowing down of supercooled liquids is related to the growth of a cooperative length scale dates back at least to Adam and Gibbs [1]. But it is only a few years back that this idea has started being substantiated by convincing experiments [2–6], numerical simulations [7–14], and simple microscopic models [15–25,27]. One of the basic problems has been to find an observable that allows one to define and measure objectively such a cooperative length scale. An interesting quantity, proposed a few years ago in the context of mean-field p-spin glasses [28] (see [29] for an important early insight) and measured in simulations, is a four-point density correlator, defined as

$$G_4(\vec{r},t) = \langle \rho(0,0)\rho(0,t)\rho(\vec{r},0)\rho(\vec{r},t)\rangle - \langle \rho(0,0)\rho(0,t)\rangle\langle \rho(\vec{r},0)\rho(\vec{r},t)\rangle, \quad (1)$$

where $\rho(\vec{r},t)$ represents the density fluctuations at position $\vec{r}$ and time t. In practice one has to introduce an overlap function w [28] to avoid a singularity due to the evaluation of the density at the same point or consider slightly different correlation functions [30]. This quantity measures the correlation in space of local-time correlation functions. Intuitively, if at point 0 an event has occurred that leads to a decorrelation of the local density over the time scale t, $G_4(\vec{r},t)$ measures the probability that a similar event has occurred a distance $\vec{r}$ away within the same time interval t (see, e.g., [31]). Therefore $G_4(\vec{r},t)$ is a candidate to measure the heterogeneity and cooperativity of the dynamics. The best theoretical justification for studying this quantity is to realize that the order parameter for the glass transition is already a two-body object—namely, the density-density correlation function $C(t)=\langle \rho(0,0)\rho(0,t)\rangle$—which decays to zero in the liquid phase and to a constant value in the frozen phase. The four-point correlation $G_4(\vec{r},t)$ therefore plays the same role as the standard two-point correlation function for a one-body order parameter in usual phase transitions. Correspondingly, the associated susceptibility $\chi_4(t)$ is defined as the volume integral of $G_4(\vec{r},t)$ and is equal to the variance of the correlation function [28,32,33]. The susceptibility $\chi_4(t)$ has been computed numerically for different model glass formers and indeed exhibits a maximum for $t=t^* \sim \tau_\alpha$, the relaxation time of the system [11–14]. The peak value $\chi_4(t^*)$ is seen to increase as the temperature decreases, indicating that the range of $G_4(\vec{r},t^*)$ increases as the system becomes more sluggish. The dynamical correlation length $\xi_4(t^*)$ extracted from $G_4(\vec{r},t^*)$ in molecular dynamics simulations grows and becomes of the order of roughly 10 interparticle distances when the time scale is of the order of 10^5 microscopic time scales τ_0 with $\tau_0 \sim 0.1$ ps for an atomic liquid. In experiments close

 ©2005 The American Physical Society

to the glass transition the dynamical correlation length has been found to be only slightly larger, between 10 and 20 interparticle distances [2,4]. This is puzzling because experiments are done on systems with relaxation times that are several orders of magnitude larger than in simulations. In fact, extrapolating simulation results in the experimental regime would lead to much larger dynamical correlation lengths. The origin of this puzzle is still unclear; see Ref. [18] for a recent discussion. Experiments on dynamical heterogeneity bridging the gap between numerical and macroscopic time scales would be extremely valuable to resolve this paradox.

Several scenarios have been proposed to understand the existence of nontrivial dynamical correlations and their relation to thermodynamical singularities. Adam and Gibbs [1], Kirkpatrick *et al.* [34] (for a different formulation, see Ref. [35]), and Kivelson and Tarjus [36] have proposed, using somewhat different arguments, the idea of collectively rearranging regions (CRR's), of size ξ, that increase as the temperature is decreased. The evolution of the system is such that these regions are either frozen or allowed to temporarily and collectively unjam for a short time until a new jammed configuration is found.

In apparent contradiction with the existence of the growing length scale, the mode-coupling theory (MCT) of glasses states that the self-consistent freezing of particles in their cages is a purely local process with no diverging length scale at the transition [37]. However, this point of view is in disagreement with the results found for mean-field disordered systems [28,29] that are conjectured to provide a mean-field description of the glass transition and display an MCT-like dynamical transition. Indeed it was recently shown that within MCT $G_4(\vec{r},t)$ in fact develops long-range correlations close to the critical MCT temperature T_c [32]. Within a phase-space interpretation of the MCT transition, the mechanism for this cooperative behavior for $T>T_c$ is the progressive rarefaction of energy lowering directions [38]. Within a real-space interpretation, the MCT transition is due to the formation of a large number of metastable states, each one characterized by a surface tension that increases from zero at T_c. As one approaches T_c from above, the relevant eigenvectors of the dynamical Hessian become more and more extended, which means that the modes of motion that allow the system to decorrelate are made of very-well-defined, collective rearrangements of larger and larger clusters of particles (see the recent work of Montanari and Semerjian [39]). For smaller temperatures $T<T_c$, "activated events" are expected to play a crucial role. They are believed to be responsible for the destruction of the freezing transition at T_c. This regime has been tentatively described by adding "hopping terms" in the MCT equations [37] or within a CRR scenario [34,35]. Note that the random first-order theory of [34] unifies MCT with CRR's predicting a first temperature regime (close to T_{MCT}) where MCT applies and then a crossover toward CRR's (the mosaic state) that describe the physical behavior close to the Kauzman temperature.

Exploiting yet a different set of ideas, models of dynamical facilitation, such as the Frederickson-Andersen [19] or Kob-Andersen models [24], have recently been proposed as paradigms for glassy dynamics [15,20,23]. In these models, the motion of particles is triggered by "mobility defects" that diffuse and possibly interact within the system. As the temperature is lowered or the density is increased, the concentration of defects goes down and the relaxation time of the system increases. The dynamics is obviously heterogeneous since it is catalyzed by defects that cannot be everywhere simultaneously. The characteristic length scale in this case is related to the average distance between defects to some model- and dimension-dependent exponent [15,18,20,23,25]. The ideas behind these models are somehow similar to the one of free-volume theories and can be traced back to the first explanation of slow dynamics in terms of defects motion [26]. Kinetically constrained models have the important merit of showing how from simple local microscopic rules a relaxation governed by the diffusion (or subdiffusion) of nontrivial defects may arise.

Understanding the mechanism behind the growth of the dynamical correlation length is certainly an important step—arguably the most important one—to understand the cause of the slowing down of the dynamics. Furthermore, the different scenarios for the glass transition can be tested, contrasting their quantitative prediction for the four-point correlation function $G_4(\vec{r},t)$ to the numerical, and hopefully soon experimental, results. Following these premises we investigate in this paper the analytical shape of $G_4(\vec{r},t)$ for several simple models. We show that $G_4(\vec{r},t)$ indeed contains some important information concerning the basic relaxation mechanisms. However, we show that, perhaps disappointingly, models where cooperativity is absent or trivial lead to four-point correlation functions and dynamical susceptibilities χ_4 that exhibit nontrivial features. Other, more complex observables will have to be defined to really grasp the nature of the collective motions involved in the relaxation process of glasses [8,40].

Let us summarize the main results of our study in terms of the susceptibility $\chi_4(t)$ and time sectors. In a supercooled liquid there are separate regimes of time scales corresponding to different physical behavior (see Fig. 1). On microscopic time scales particles move ballistically if the dynamics is Newtonian or diffusively if the dynamics is Brownian. On a longer time scale, interactions start playing a role, which can be described approximately using elasticity theory, before a truly collective phenomenon sets in. This nontrivial glassy regime is the β regime, within which correlation functions, such as, for example, the dynamical structure factor, develop a plateau. The β regime is divided further in an early- and a late-β regime corresponding, respectively, to the approach and departure from the plateau of the correlation function. Finally the structural relaxation time scale on which correlation functions decay to zero is the α regime. All previous studies have focused on the behavior of $\chi_4(t)$ at times of the order of τ_α which correspond to the peak of $\chi_4(t)$. We show that $\chi_4(t)$ has in fact a rich structure in time and different behavior in different time sectors. In many of these regimes, $\chi_4(t)$ behaves as a power law of time t^μ with different values of μ. During the ballistic time scale one finds $\mu=4$ ($\mu=2$ for Brownian dynamics), whereas during the elastic regime (most relevant deep in the glass phase), the exponent becomes $\mu=1$ for ballistic phonons and $\mu=1/2$ for

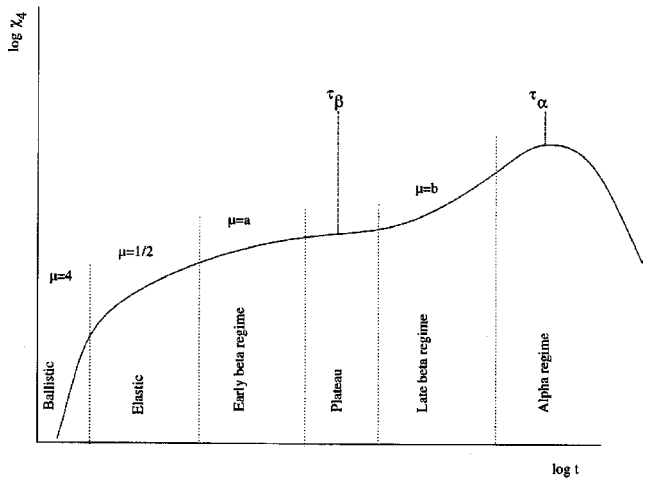

FIG. 1. Sketch of the time behavior of $\chi_4(t)$, with all the different time regimes, within the MCT description that we find to be a good description around T_c. As the temperature is lowered, we expect the elastic regime to extend up to τ_α.

diffusive phonons. The behavior in the β and α regimes is intimately related to the physical mechanism for relaxation and indeed we find quite different answers depending on which scenario we focus on. MCT predicts exponents $\mu=a$ and $\mu=b$ on time scales corresponding, respectively, to the early- and late-β regimes, where a and b are the standard MCT exponents obtained from the study of the dynamical structure factor. The power law t^b extends until the peak in $\chi_4(t)$ is reached.

The other scenarios only make predictions in the α regime. In the case of CRR's one has $\chi_4 \sim t$ or $\chi_4 \sim (\ln t)^{d+1/\psi}$ before the peak depending whether one assumes that the relaxation occurs via bulk nucleation events or domain wall fluctuations; see below. For diffusing defects in dimension $d=3$, the exponent is $\mu=2$. If defects have a nontrivial diffusion exponent z, such that their displacement at time t scales as $t^{1/z}$, then $\mu=2d/z$ for $d<z$ and $\mu=2$ otherwise. The overall behavior of $\chi_4(t)$ is summarized by Fig. 1, which specializes to the MCT predictions for simplicity.

Another important feature of χ_4 is the growth of the peak compared to the growth of the time $t=t^* \sim \tau_\alpha$ at which the peak takes places [21]. This is found to scale as $\chi_4(t^*) \sim t^{*\lambda}$, with $\lambda=0$ (logarithm) for CRR's, $\lambda=1$ for freely diffusing defects, $\lambda=d/z$ for anomalously diffusing defects for $d<z$, and $\lambda=1$ again for $d>z$. Note that if the defect diffusion coefficient itself scales with t^* as $1/t^{*f}$, such as, for example, in the one-spin facilitated FA model, there is an extra contribution that gives $\lambda=1-f$ for $d>z$. Finally, one has $\lambda=1/\gamma$ in the context of MCT, where γ describes the power-law divergence of the relaxation time as the critical MCT temperature is approached.

We have checked these predictions in two model systems of glass-forming liquids: a Lennard-Jones and a soft-sphere mixture. Concerning the behavior of $\chi_4(t)$ in the late-β and -α regimes, the most interesting time sectors, we have found reasonable agreement with the MCT predictions for four point correlators. This agreement is by no means trivial and is actually quite unexpected unless MCT indeed captures some of the physics of the problem. Instead models of diffusing, defects do not describe well the numerical results. This is perhaps not very surprising since we are focusing on two fragile liquids (at least in the numerical time window) at temperatures well above the experimental glass transition. It might be that the predictions of these models work only on larger time scales. In any case, we expect instead that for strong liquids displaying an Arrhenius behavior the predictions for $\chi_4(t)$ obtained studying the model of simple diffusing defects might hold quantitatively, since it seems quite well established from numerical simulations that relaxation in strong liquids is triggered by the diffusion of connectivity defects [41,42]. Finally, the CRR picture does not agree quantitatively with our present numerical data. However, this picture is supposed to describe the liquid dynamics precisely in the low-temperature and long-time regime, which is presently beyond numerical capabilities. Again, experimental results probing the behavior of $\chi_4(t)$ in this regime would be highly valuable to put strong constraints on the different theoretical scenarios of glass formation.

The organization of the paper is as follows. In Sec. II we discuss the behavior of $\chi_4(t)$ on microscopic time scales. Then, we analyze the predictions of elasticity theory in Sec. III. In Secs. IV and V we focus on the behavior of $\chi_4(t)$ in the β and α regimes for MCT and CRR's. In Sec. VI we discuss the predictions of defect models analytically using an independent defect approximation and by numerical simulations of kinetically constrained models. In Sec. VII we compare the different predictions to the results of numerical simulations of models of glass-forming liquids. We present our conclusions in Sec. VIII.

II. MICROSCOPIC DYNAMICS

On very short time scales the behavior of χ_4 can be computed exactly. For simplicity, we characterize the dynamics through the self-intermediate scattering function

$$F_s(k,t) = \frac{1}{N}\sum_i \langle \cos \vec{k} \cdot [\vec{r}_i(t) - \vec{r}_i(0)] \rangle \tag{2}$$

and define the dynamic susceptibility as the variance of the fluctuations of $F_s(k,t)$:

$$\chi_4(t) = N\left[\left\langle \left(\frac{1}{N}\sum_i \cos \vec{k} \cdot [\vec{r}_i(t) - \vec{r}_i(0)] \right)^2 \right\rangle - \left\langle \frac{1}{N}\sum_i \cos \vec{k} \cdot [\vec{r}_i(t) - \vec{r}_i(0)] \right\rangle^2 \right]. \tag{3}$$

The full intermediate four-point scattering function defined in Eq. (1) in fact contains very similar information, even for interacting systems—as shown by numerical simulations [12,13].

On a very short time scale particles move ballistically if the dynamics is Newtonian, $\vec{r}_i(t) - \vec{r}_i(0) = \vec{v}_i t + O(t^2)$, where $\vec{v}_i$ is the velocity of the particle i at time t. Since the system is in equilibrium all the $\vec{v}_i$'s are independent Gaussian variables with variance $\langle \vec{v}_i \cdot \vec{v}_j \rangle = \delta_{ij} 3k_B T/m$, where T is the tempera-

ture, m the mass of the particles, and k_B the Boltzmann constant. Using this property it is straightforward to obtain

$$F_s(k,t) = \exp\left(- \vec{k}^2 \frac{k_B T}{2m} t^2 \right) \tag{4}$$

and

$$\chi_4(t) = F_s(k,t)^2 \left[\cosh\left(- 2\vec{k}^2 \frac{k_B T}{m} t^2 \right) - 1 \right]. \tag{5}$$

For an interacting particle systems this is only valid on short time scales—for example, smaller than the collision time for short-ranged interactions. This leads to an initial power-law increase that reads

$$\chi_4(t) = \frac{1}{2} (\vec{k}^2)^2 \left(\frac{k_B T}{m} \right)^2 t^4 + O(t^6). \tag{6}$$

Note that if one had chosen Langevin dynamics (i.e., $\partial_t \vec{r}_i = \partial_{\vec{r}} H + \vec{\eta}_i$) instead of Newtonian dynamics, Eqs. (5) and (6) would have been identical except for the replacement of $k_B T t^2/m$ by $2Tt$, again for small times. Thus changing from Newtonian to Langevin dynamics, the initial power-law increase of $\chi_4(t)$ changes from t^4 to t^2. This is similar to the change in the mean-square displacement that increases as t^2 and t, respectively, for Newtonian and Langevin dynamics.

In the above example, however, it is clear that the increase of χ_4 with time has nothing to do with the increase of a correlation length, since particles are assumed to be independent. In other words, the four-point correlation $G_4(\vec{r},t)$ has a trivial δ-function spatial dependence, but the height of the δ peak increases with time. As will be discussed later in the paper, it is important to normalize $\chi_4(t)$ by the value of $G_4(\vec{r}=0,t)$ to conclude from the four-point susceptibility that a length scale is indeed growing in the system.

III. ELASTIC CONTRIBUTION

For longer time scales the interaction between particles starts playing a role. Generically one expects that in the time regime where the displacements of particles remain small, an elastic description should be valid. In a solid or in a glass deep below T_g, there is no further relaxation channels and the elastic contribution to χ_4 should be the only relevant one. In a supercooled liquid around the mode-coupling temperature T_c, the elastic regime is interrupted by the collective β regime, where in some sense phonon-phonon interactions completely change the physical picture. Although we expect such a crossover, we have at present no detailed theoretical description of it.

In the following we analyze again the behavior of the four-point self-intermediate scattering function assuming that the dynamical behavior of the liquid can be described, within a restricted time sector, as an elastic network (we will discuss later how to include, in a phenomenological way, viscous flow). Perhaps surprisingly, we find a nontrivial structure for G_4 in this model, with an ever growing "cooperative" length scale which comes from the dynamics of phonons, which represents the simplest form of cooperativity.

We consider an isotropic solid immersed in a viscous thermal bath. The energy of the system is given by

$$H = \int d^d r \frac{1}{2} \kappa_1 \left[\sum_i u_{ii} \right]^2 + \kappa_2 \sum_{i,j} u_{i,j}^2, \tag{7}$$

where κ_1, κ_2 are the Lamé coefficient, $u_{i,j} = \frac{1}{2}[d\phi_i/dx_j + d\phi_j/dx_i]$ is the deformation tensor, and $\vec{\phi}$ the displacement field from an undeformed reference state. Note that $\vec{\phi}(x)$ is simply the continuum limit of the displacement of each particle with respect to its equilibrium (bottom of the well) position.

As is well known, the above energy leads to three independent phonon modes (one longitudinal and two transverse modes). For simplicity, we only consider one deformation mode and write the Hamiltonian in Fourier space as

$$H = \frac{1}{2} \kappa \int \frac{d^d k}{(2\pi)^d} k^2 \phi_k \phi_{-k}, \tag{8}$$

where κ is an effective elasticity modulus. The mode k has an energy $E_k = \kappa k^2 \phi_k \phi_{-k}/2$ and therefore we expect, in equilibrium, $\langle \phi_k \phi_{-k} \rangle = T/\kappa k^2$, where the Boltzmann constant has been set to unity. Our goal is to calculate the dynamical correlation functions of the system. We describe the dynamics by a Langevin equation with a local noise:

$$m \frac{\partial^2 \phi(\vec{r},t)}{\partial t^2} + \nu \frac{\partial \phi(\vec{r},t)}{\partial t} = \kappa \Delta \phi(\vec{r},t) + \zeta(\vec{r},t), \tag{9}$$

where $\zeta(x,t)$ is a Gaussian noise uncorrelated in space and time, of variance equal to $2\nu T$. Taking the Fourier transform

$$m \frac{\partial^2 \phi_k}{\partial t^2} + \nu \frac{\partial \phi_k}{\partial t} = - \kappa k^2 \phi_k + \zeta_k(t), \tag{10}$$

$\zeta_k(t)$ is again a Gaussian noise uncorrelated for different k's and time.

In this section, we only consider in details the overdamped case $m=0$ and set $D=\kappa/\nu$, but also give at the end the result for the purely propagative case $\nu=0$ (see also Appendix A). One easily deduces the non-equal-time correlation in the overdamped case:

$$\langle \phi_k(t) \phi_{-k}(0) \rangle = \frac{T}{\kappa k^2} e^{-Dk^2 t}. \tag{11}$$

Let us now define the function

$$F^{(q)}(r,t) = \sum_i \delta(r - r_i(0)) \cos\{q[r_i(t) - r_i(0)]\}, \tag{12}$$

whose average equals the self-intermediate scattering function up to a constant (the particle density).

Using the microscopic definition of $\vec{\phi}$ we obtain that

$$C(q,t) = \langle F^{(q)}(r,t) \rangle \simeq \langle e^{iq[\phi(\vec{r},t) - \phi(\vec{r},0)]} \rangle = e^{-q^2 \langle [(\phi(\vec{r},t) - \phi(\vec{r},0)\ ]^2 \rangle/2}, \tag{13}$$

where the last equality comes from the Gaussian nature of the deformation field. Using the above results on the correlation of the Fourier modes, we find

$$\langle[\phi(\vec{r},t)-\phi(\vec{r},0)]^2\rangle = \frac{2T}{\kappa}\int \frac{1-e^{-Dk^2t}}{k^2}\frac{d^dk}{(2\pi)^d}. \quad (14)$$

As is well known, this integral behaves differently for $d \leqslant 2$ and for $d>2$, reflecting the fact that phonons destroy translational order in low dimensions. As above, we will only consider here the physical case $d=3$, relegating the discussion of the other cases to Appendix A. For $d=3$, we need to introduce an ultraviolet cutoff Λ on the wave vector k, which is the inverse of the underlying lattice spacing a. Then, the above integral goes to a constant $\propto\Lambda$ at large times, reflecting the fact that particles are localized in their "cage." Therefore, the self-intermediate scattering function $C(q,t)$ decays at small times $\Lambda^2 Dt \ll 1$ before saturating to a "plateau" value given by

$$f_q \equiv C(q,t\to\infty) = \exp\left(-c\frac{T\Lambda q^2}{\kappa}\right), \quad (15)$$

where c is a numerical constant. (Note that $T\Lambda q^2/\kappa$ has no dimension and is expected, from a Lindemann criterion, to be of the order of 0.05 at half the melting temperature and for $q=\Lambda$.) In real glass-forming liquids, this plateau phase does not persist forever, and $C(q,t)$ finally decays to zero beyond $t=\tau_\alpha$, in the so-called α-relaxation regime. A modification of the model to account for this decorrelation will be discussed later. Furthermore, the above pseudo-β regime predicted by elastic theory does not explain quantitatively the β regime in supercooled fragile liquids, except probably on relatively short time scales—say, up to a few picoseconds. On the other hand, at temperatures below T_g or for strong glasses, we expect that the elastic regime will extend up to τ_α and compete with other mechanisms, such as the defect-mediated correlation discussed in Sec. VI below.

The calculation of $G_4^{(q)}(\vec{r},t)=\langle F^{(q)}(r',t)F^{(q)}(r'+r,t)\rangle_c$ is detailed in Appendix A. One immediately sees that $G_4^{(q)}(\vec{r},t)$ is governed by a diffusive correlation length $\xi(t) \sim \sqrt{Dt}$ with $D=\kappa/\nu$, as expected from the structure of the Langevin equation that describes relaxational dynamics. Clearly, in the case of propagative phonons, one finds $\xi(t) \sim Vt$ with $V^2=\kappa/m$. The final result, see Appendix A, is

$$G_4^{(q)}(\vec{r},t) = C^2(q,t)\{\cosh[2q^2R(\vec{r},t)]-1\}, \quad (16)$$

where

$$R(\vec{r},t) = \frac{T}{\kappa}(Dt)^{1-d/2}F\left(\frac{r}{\sqrt{Dt}}\right) \quad (17)$$

and we find (see Appendix A) $F(z)\simeq(4\pi z)^{-1}$ for $z\ll 1$ and $F(z)\simeq(2\pi^{3/2})^{-1}\exp(-z^2/4)/z^2$ for $z\gg 1$. Note the similarity between the expression in Eq. (16) and the corresponding one (5) derived in the previous section. One can check that indeed the short-time behavior is indeed the one derived before in the case of Langevin dynamics for the particles, as expected. Let us now focus on long times, but still within the elastic regime, $\Lambda^2 Dt \gg 1$, and for $r \ll \xi(t)$,

$$G_4^{(q)}(\vec{r},t) = f_q^2\left[\cosh\left(\frac{Tq^2}{2\pi\kappa r}\right)-1\right]. \quad (18)$$

Suppose for simplicity that we are in a regime where the argument of the cosh is always small, corresponding to the limit $Tq^2\Lambda \ll \kappa$ (remember that by definition $r>a=2\pi/\Lambda$, where a is the interatomic distance). Then, $G_4(\vec{r},t)\sim r^{-2}$ for $\Lambda^{-1}\ll r \ll \xi(t)$. For larger scales $r\gg\xi(t)$ decays as a Gaussian—i.e., superexponentially fast. Note that the small-r behavior of $G_4(\vec{r},t)$ is not of the Ornstein-Zernike form ($1/r$ in $d=3$). Integrating G_4 over $\vec{r}$ we find the dynamical susceptibility

$$\chi_4^{(q)}(t) \sim \frac{T^2q^4f_q^2}{\kappa^2}\xi(t). \quad (19)$$

This result is actually valid both for in the diffusive limit where $\xi(t)=\sqrt{Dt}$ and in the propagative regime where $\xi(t)=Vt$. Therefore $\chi_4^{(q)}(t)$ increases either as $\sqrt{t}$ or as t (note that in the limit of small times one recovers the t^4 or t^2 laws obtained in the previous section). In the general case, one expects a crossover between a propagative regime at small times $t<m/\nu=D/V^2$ (of the order of ps in glass formers; see [43]) and a diffusive regime for longer time scales. Thus, looking at $\chi_4^{(q)}(t)$ as a function of time in a log-log plot one should see first a straight line corresponding to the ballistic or diffusive motion leading, respectively, to slope $\mu=4$ or $\mu=2$, bending over toward a smaller slope (1 or 1/2, or both, depending on the strength of the dissipation). The order of magnitude of $\chi_4^{(q)}(t)$, as given by Eq. (19), can be estimated to be $\sim(10^{-3}-10^{-2})a^2\xi(t)$ for $q=\Lambda$. In the propagative regime with $t=1$ ps, $V=3\times10^3$ m/s, and $a=0.3$ nm, one finds $\xi=10a$ and $\chi_4^{(q)}\sim(10^{-2}-10^{-1})a^3$—i.e., a small, but perhaps detectable signal from the phonons. Only on much larger time scales will the elastic contribution be significant, a regime that can be reached deep in the glass phase [44]. As mentioned above, other collective modes come into play in supercooled fragile liquids, in particular around the mode-coupling temperature, and give rise to the β regime where "cages" themselves become more complex, extended objects [32].

The above calculation shows that in an elastic solid with diffusive or propagative phonon modes, the dynamical susceptibility increases without bound, reflecting the presence of Goldstone soft modes in the system. Of course, in a real glass the correlation function $C^{(q)}(t)$ eventually decays to zero beyond the α-relaxation time τ_α, as particles start diffusing out of their cages, far away from their initial position. If phonons were the only relevant excitations, this would cause the dynamical susceptibility to peak around $t=t^*=\tau_\alpha$. A phenomenological model that describes the decay of $\chi_4^{(q)}(t)$ within the above elastic framework is to assume a (Maxwell) viscoelastic local modulus:

$$\frac{\partial\phi(\vec{r},t)}{\partial t} = \kappa\left[\int_{-\infty}^{t} dt' e^{-\gamma(t-t')}\Delta\frac{\partial\phi(\vec{r},t')}{\partial t'}\right] + \zeta(\vec{r},t), \quad (20)$$

with $\gamma\sim\tau_\alpha^{-1}$, corresponding to a frequency-dependent elastic modulus $\kappa(\omega)=i\kappa\omega/(i\omega+\gamma)$. In this model, the dynamics of

ϕ becomes diffusive at times $>\gamma^{-1}$ and the dynamic structure factor therefore decays exponentially beyond that time. Of course, the model itself becomes inconsistent at large times, since the underlying lattice needed to define the deformation field ϕ has by then totally melted.

The conclusion of this section, however, is that since supercooled liquids behave at high frequencies ($\omega \gg \gamma, \tau_\alpha^{-1}$) like solids, the four-point correlation and dynamical susceptibility are expected to reveal, in a certain time domain, a nontrivial behavior unrelated to the structure of the "collective processes" discussed below (MCT, diffusive defects, CRR's) that one usually envisions to explain glassy dynamics.

IV. MODE-COUPLING THEORY

As mentioned in the Introduction the mode-coupling theory of supercooled liquids predicts the growth of a cooperative length as the temperature is decreased or the density increased [28,29,32] and makes detailed predictions on the shape of $\chi_4(t)$. The four-point correlation function becomes critical near the mode-coupling transition temperature T_c. The behavior of the susceptibility $\chi_4(t)$ is encoded in ladder diagrams [29,32]. From the analytical and numerical results of [32] and analyzing the ladder diagrams [32,45], we have found that, in the β regime,

$$\chi_4(t) \sim f_1(t\epsilon^{1/2a})/\sqrt{\epsilon}, \quad t \sim \tau_\beta, \tag{21}$$

and in the α regime,

$$\chi_4(t) \sim f_2(t\epsilon^{1/2a+1/2b})/\epsilon, \quad t \sim \tau_\alpha, \tag{22}$$

where $\epsilon = T - T_c$, a, b, and $\gamma = 1/2a + 1/2b$ are the MCT exponents for the dynamical structure factor, and $f_1(x)$ and $f_2(x)$ are two scaling functions. Requiring that the dependence on ϵ drop out when $t\epsilon^{1/2a} \ll 1$ one finds that $f_1(x) \sim x^a$ when $x \ll 1$. This leads to a power-law behavior $\chi_4 \sim t^a$ in the early-β regime—i.e., when the intermediate scattering functions approaches a plateau. In the same way, matching the behavior of f_1 when $x \gg 1$ to the one of f_2 when $x \ll 1$ one finds another power-law behavior $\chi_4 \sim t^b$ on time scales between the departure from the plateau and the peak of χ_4. We give in Fig. 1 a schematic summary of the shape of $\chi_4(t)$ within the MCT description of supercooled liquids.

Finally, as discussed in [32], at times $t = t^* \sim \tau_\alpha$, χ_4 reaches a maximum of height $(T - T_c)^{-1}$. Using the relation $\tau_\alpha \sim (T - T_c)^{-\gamma}$, valid within MCT, one finally finds $\chi_4(t^*) \sim t^{*1/\gamma}$.

Note that all the predictions made above are valid in the microcanoncial NVE ensemble, see [45] for a further discussion.

V. COLLECTIVELY REARRANGING REGIONS

Under the term CRR, we gather many similar scenarios that differ in their details, as discussed in the Introduction [1,34–36]. Within the frustration-limited domains scenario of Ref. [36] it seems natural to envision the dynamics as the activated motion of domains pinned by self-generated disorder. In the case of the random first-order theory of Refs. [34,35], the details of the decorrelation mechanism are not entirely clear. There should be, on the one hand, activated fluctuations of domain walls between different states, again pinned by self-generated disorder. However, the fluctuations leading to a change of state may be the nucleation of a completely different state starting from the bulk. The latter process can be modeled as a nearly instantaneous event with a certain (small) nucleation rate. In the following we shall analyze separately these two types of fluctuations and their consequences on the shape of $\chi_4(t)$.

A. Instantaneous events

Suppose that the dynamics is made of nearly instantaneous events that decorrelate the system in a compact "blob" of radius ξ_0. The probability per unit time and volume for such an event to appear around site $\vec{r}$ is Γ. We compute the four-body correlation of the persistence, $n_r(t)$, defined to be equal to one if no event happened at $\vec{r}$ between times 0 and t and equal to zero otherwise. The four-body correlation is then defined as

$$G_4(\vec{r},t) = \langle n_r(t) n_0(t) \rangle - \langle n_r(t) \rangle^2. \tag{23}$$

Clearly, the averaged correlation function $C(t) = \langle n_r(t) \rangle$ is simply given by $C(t) = \exp(-\Omega\Gamma\xi_0^d t)$ where Ω is the volume of the unit sphere. For $G_4(\vec{r},t)$ to be nonzero, an event must have happened simultaneously at $\vec{r}$ and at 0, leading to

$$G_4(\vec{r},t) = C^2(t)\{\exp[\Gamma t \xi_0^d f(r/\xi_0)] - 1\}, \tag{24}$$

where $f(x)$ is the volume of the intersection between two spheres of unit radius with centers at distance x apart. Clearly, $f(x>2) = 0$. Therefore, $G_4(\vec{r},t)$ is nonzero only if $r < 2\xi_0$, and is in fact roughly constant there. For a given r satisfying this bound, G_4 first grows linearly with time, reaches a maximum for $t = t^* \approx \Gamma^{-1}\xi_0^{-d}$ and decays exponentially beyond that time. The same behavior is found for $\chi_4(t)$, which grows initially as t^μ with $\mu = 1$ and reaches a maximum such that $\chi_4(t^*) \propto \xi_0^d$. Assuming finally that these events are activated [34,35], with a barrier growing like $\Upsilon\xi_0^\psi$, where ψ is a certain exponent, one expects $t^* \sim \tau_0 \exp(\Upsilon\xi_0^\psi/T)$, and therefore $\chi_4(t^*) \propto (\ln t^*)^{d/\psi} \propto \xi_0^d$.

The rearranging regions could have of course more complicated shapes than the simple sphere assumed above. As long as these objects are reasonably compact, the above results will still hold qualitatively. On the other hand, if these regions are fractal with a dimension $d_f < d/2$, the above results on G_4 will hold with the argument in the exponential given by $\Gamma t r^{2d_f - d}$; one also finds $t^* \approx 1/\Gamma\xi_0^{d_f}$ and $\chi_4(t^*) \propto \xi_0^{d_f}$.

B. Domain wall fluctuations

In this case the picture that we have in mind is similar to the case of a disordered ferromagnet with pinned domain walls, where the typical time to flip a domain is comparable to the interevent time. In that case, an "event" is in fact the slow fluctuation of domain walls that progressively invade the bulk of the domain [in the follow we neglect the fast equilibrium dynamics taking place inside the domains that determines the evolution of $\chi_4(t)$ on short time scales]. The

early-time behavior of $\chi_4(t)$ is given by the square of the number of particles that relax per unit volume thanks to the same domain wall (see [31] for the same situation out of equilibrium in pure systems).[1] Let again ξ_0 be the typical size of a domain and $\ell(t)$ the length scale over which the domain walls fluctuate during time t. Considering that on the surface of each domain there are order $(\xi_0/\ell)^{d-1}$ subdomains of linear size ℓ and that the number of particles in each of these subdomains is proportional to ℓ^d, we get $\chi_4(t) \propto \xi_0^{-d}(\xi_0/\ell)^{d-1}\ell^{2d} \propto \ell^{d+1}/\xi_0$. We are descarding for simplicity both the possibility of fractal domains and that transverse fluctuations behave differently from longitudinal ones. Assuming thermal activation over pinning energy barriers that grow like $\Upsilon\ell^{\psi}$ [46], we finally get $\chi_4(t) \propto \xi_0^{-1}(\ln t)^{d+1/\psi}$. Therefore, in this case, the exponent μ is formally zero and the growth of $\chi_4(t)$ is only logarithmic. The maximum of χ_4 occurs at time t^* such that $\ell(t^*) \approx \xi_0$, which implies that the maximum of the susceptibility also scales logarithmically with t^*, $\chi_4(t^*) \propto \xi_0^{-1}(\ln t^*)^{d+1/\psi} \propto \xi_0^d$. The same scaling of the maximum of the susceptibility with the typical domain size is obtained in nondisordered coarsening systems [31].

The conclusion of the above analysis is that if the CRR relaxation is due to both instantaneous events and domain wall fluctuations, the latter will dominate the time behavior of χ_4 before the peak as can be readily deduced by comparing their relative contributions to $\chi_4(t)$. If for some reason domain walls are particularly strongly pinned and bulk nucleation becomes dominant, then the exponent $\mu=1$ should be observable. The height of the peak, on the other hand, behaves identically in both models. Thus, as the temperature is reduced, one should see a power-law behavior before the peak with an exponent $0<b<1$ in the MCT regime followed by an effective exponent μ either decreasing toward zero or increasing toward one depending on whether the domain wall contribution dominates or not. However, at lower temperatures, the elastic contribution will also start playing a role, which might completely dominate over the CRR contribution. This suggests that other observables, which quantify more specifically the collective dynamics, should be devised to reveal a CRR dynamics.

VI. DEFECT-MEDIATED MOBILITY

A. Independently diffusing defects

As the simplest realization of the defect-mediated scenario for glassy dynamics advocated in [15,16,19,20,24], we consider a lattice model in which mobility defects, or vacancies, perform independent symmetric random walks. We assume for the moment that these vacancies cannot be created or destroyed spontaneously. We shall compute the same function $G_4(\vec{r},t)$ as in Eq. (23) above, arguing that when such a vacancy crosses site $\vec{r}$, the local configuration is reshuffled and the local correlation drops to zero. Therefore, $n_r(t)$ is equal to one, if no vacancy ever visited site $\vec{r}$ between $t=0$ and t, and zero otherwise. Thus, $\langle n_r(t)\rangle$ represents a density-density dynamical correlation function whereas $\langle n_0(t)n_{\vec{r}}(t)\rangle - \langle n_0(t)\rangle^2$ corresponds to $G_4(\vec{r},t)$.

From now on we will denote by N_v the number of vacancies, by V the total volume, by $\rho_v = N_v/V = 1-\rho$ the vacancy density and by $P_x^z(t)$ the probability that a vacancy starts in z at time zero and never reaches x until time t. The probability that a vacancy starts in z at time zero and reaches for the first time x at a time $u \leqslant t$ is therefore $P_x^z(t) = 1 - P_{\bar{x}}^z(t)$.

The computation of $\langle n_x(t)\rangle$ is identical to the target annihilation problem considered in [47]. Since we assume defects to be independent, the defect distribution is uniform and we have

$$\begin{aligned}\langle n_x(t)\rangle &= \left[\frac{1}{V}\sum_{z,z\neq x} P_{\bar{x}}^z(t)\right]^{N_v} \\ &= \left[\frac{1}{V}\sum_{z,z\neq x}(1-P_x^z(t))\right]^{N_v} \\ &= \exp\left[-\rho_v - \rho_v \sum_{z,z\neq x} P_x^z(t)\right]. \end{aligned} \tag{25}$$

The correlation function $\langle n_x(t)n_y(t)\rangle$ can be also expressed in terms of probability distributions of a single random walk in a similar way:

$$\begin{aligned}\langle n_x(t)n_y(t)\rangle &= \left[\frac{1}{V}\sum_{z,z\neq x,y} P_{\overline{x,y}}^z(t)\right]^{N_v} \\ &= \left[\frac{1}{V}\sum_{z,z\neq x,y}[1-P_x^z(t)-P_{y,\bar{x}}^z(t)]\right]^{N_v} \\ &= \left[1-\frac{2}{V}-\frac{1}{V}\sum_{z,z\neq x,y}P_x^z(t)-\frac{1}{2V}\right. \\ &\quad \left.\times\sum_{z,z\neq x,y}[P_{y,\bar{x}}^z(t)+P_{x,\bar{y}}^z(t)]\right]^{N_v} \\ &= \exp\left(-2\rho_v-\rho_v\sum_{z,z\neq x}P_x^z(t)+\rho_v P_x^y(t)\right. \\ &\quad \left.-\frac{\rho_v}{2}\sum_{z,z\neq x,y}[P_{y,\bar{x}}^z(t)+P_{x,\bar{y}}^z(t)]\right) \end{aligned} \tag{26}$$

where $P_{\overline{x,y}}^z(t)$ is the probability that a vacancy starts in z at time zero and never reaches either x or y until time t and $P_{x,\bar{y}}^z(t)$ is the probability that a vacancy starts in z at time zero and reaches x at $u \leqslant t$ but never reaches y until time t. In Eqs. (25) and (26) we are left with the calculation of probabilities of the form $P_x^z(t)$, $P_{x,\bar{y}}^z(t) + P_{y,\bar{x}}^z(t)$ for a single random walk. This can be done using Laplace transforms and, concerning $P_x^z(t)$, the computation has been performed a while ago [48]. All the details can be found in Appendix B.

In the continuum limit, $(x-y)/\sqrt{Dt/2} \sim O(1)$; i.e., for independent Brownian motion with diffusion coefficient D, the final expression for $\langle n_x(t)\rangle$ on time scales much larger than one is, in three dimensions,

[1] We are implicitly assuming that the variance of N_α, the number of particles that relax per unit volume thanks to the same domain wall, equals the square of the average N_α

$$\langle n_x(t)\rangle = \exp[-\rho_v - c_1 D\rho_v t], \tag{27}$$

where c_1 is a constant fixed by the short-length-scale physics—i.e., the underlying lattice structure (see Appendix B). It is clear from this expression which is valid in all dimensions larger than 2 that the relaxation time scale is governed by the vacancy density ρ_v and reads $\tau = 1/(c_1\rho_v D)$. Physically τ corresponds to the time such that each site has typically been visited once by a defect.

The final expression for G_4 is, for time and length scales much larger than 1, and in the small vacancy density limit $\rho_v \to 0$,

$$G_4(\vec{r},t) = \frac{c_2}{\rho_v}\exp\left(-\frac{2t}{\tau}\right)\left(\frac{t}{\tau}\right)^2 \int_0^1 du \int_0^u dv \frac{e^{-r^2/2Dvt}}{(2\pi Dvt)^{3/2}}, \tag{28}$$

where c_2 is a constant of order unity. Note that the correlation length at fixed t is given by $\xi(t) = \sqrt{Dt}$. For $r \ll \xi(t)$, $G_4(\vec{r},t) \sim 1/r$, whereas for $r \gg \xi(t)$, G_4 decays at leading order as a Gaussian—that is, much faster than exponentially. The $1/r$ behavior is cut off on short-length scales, where Eq. (28) does not hold. For $r=0$ one finds, when $t \gg 1$,

$$G_4(r=0,t) = \langle n_x(t)\rangle - \langle n_x(t)\rangle^2 = \exp(-t/\tau)[1-\exp(-t/\tau)], \tag{29}$$

which behaves as t/τ at small times.

By integrating Eq. (28) over $\vec{r}$ we get the dynamical susceptibility

$$\chi_4(t) = \frac{c_2}{2\rho_v}\left(\frac{t}{\tau}\right)^2 \exp\left(-\frac{2t}{\tau}\right). \tag{30}$$

For short times $t < \tau$, the dynamical susceptibility is proportional to t^2, so that $\mu = 2$. This is due to the diffusing nature of the defects. The main contribution to χ_4 is given by the square of the number of sites visited by the same defect, which behaves as $\rho_v(Dt)^2 = (1/\rho_v)(t/\tau)^2$, since a random walk in three dimensions typically visits t different sites. For $t > \tau$, on the other hand, the correlation decreases because sites start being visited by different vacancies. The maximum of $\chi_4(t)$ is reached for $t = t^* = \tau$, for which one has $\chi_4(t^*) \sim \rho_v^{-1} \sim Dt^*$. Note that because random walks are fractals of dimension $d_f = 2$, the above relation can also be written as $\chi_4(t^*) \sim a^{d-d_f}\xi^{d_f}(t^*)$, where we have added the lattice spacing a to give to χ_4 the dimension of a volume. If for some reason D depends on ρ_v, as happens, for example, for the one-spin-facilitated Fredrickson-Andersen (FA) model where $D \propto \rho_v$, then one finds $t^* \sim \rho_v^{-2}$ and $\chi_4(t^*) \sim t^{*1/2}$.

Taking the Fourier transform of $G_4(r,t)$ given by Eq. (28), we find the four-point structure factor $S_4(k,t)$,

$$S_4(k,t) = \chi_4(t)\mathcal{F}(Dk^2t), \quad \mathcal{F}(u) \equiv \frac{2}{u^2}(u-1+e^{-u}). \tag{31}$$

Note that $S(k=0,t) = \chi_4(t)$, as it should. Furthermore, for large and small k, $S_4(k,t)$ behaves, respectively, as $S_4 \sim k^{-2}$ and $S_4 \sim \chi_4 + O(k^2)$, just as the Ornstein-Zernike form, though the detailed k dependence is different.

One can also study this problem in dimension $d=1$ or $d=2$. Qualitatively, the same conclusions hold (diffusive correlation length $\sqrt{Dt}$, correlation time t^* set by the density of vacancies, etc.), although the quantitative results differ because a random walk in $d \leqslant 2$ visits a number of sites that grows sublinearly with time; see Appendix B 1 and B 3. One finds in particular that $\chi_4(t^*) \sim (Dt^*)^{d/2} \sim \xi^d(t^*)$, with logarithmic corrections for $d=2$. The above arguments can be generalized if for some reason the vacancies have an anomalous diffusion motion, in the sense that their typical excursion between time $t=0$ and time t scales as $t^{1/z}$, where z is the dynamical exponent. When $z=2$, the usual diffusion is observed, but many models like diffusion in random media or kinetically constrained models may lead to subdiffusion, where $z > 2$ [21,49]. In this case, one expects the small-time behavior of $\chi_4(t)$ to be given by $\chi_4(t) \sim t^{2d/z}$ for $d < z$ and t^2 for $d > z$ with logarithmic corrections for $d=z$. Similarly, the behavior of $\chi_4(t^*)$ is a power law $\chi_4(t^*) \sim t^{*\lambda}$, with $\lambda = d/z$ for $d < z$ and $\lambda = 1$ for $d > z$.

In the above model, mobility defects were assumed to be conserved in time. However, it is certainly more realistic to think that these defects can be spontaneously created and disappear with time. Suppose that defects are created with a rate Γ per unit time and unit volume and disappear with a rate γ per unit time. The equilibrium density of defects is then $\rho_v = \Gamma/\gamma$. The above results on χ_4 can easily be generalized. At small times, the number of pairs of visited sites will now behave as $\rho_v(Dt)^2 - \frac{2}{3}\Gamma(Dt)^3/D$. Because of the death of vacancies, there is an extra decay of the dynamical susceptibility. The dominant rate of decay depends on the adimensional number $\gamma\tau$.

A very similar model for glassy dynamics was suggested in [50], where free volume is described as a diffusing coarse-grained density field $\rho(\vec{r},t)$ with a random Langevin noise term. Mobility of particles is allowed whenever the density ρ exceeds a certain threshold ρ_0. The mobile regions are then delimited by the contour lines of a random field, which already gives rise to a quite complex problem of statistical geometry [51]. The particle density correlation in this model is a simple exponential with relaxation time $\tau \sim \exp(\rho_0/\overline{\rho})$, where $\overline{\rho}$ is the average free-volume density. One can also compute $\chi_4(t)$ in this model to find, in $d=3$,

$$\chi_4(t) \sim t\left\{\exp\left(-\frac{t}{\tau}\right)\left[1-\exp\left(-\frac{t}{\tau}\right)\right]\right\}, \tag{32}$$

which behaves very much like the pointlike vacancy model studied above, with in particular, $\chi_4(t) \sim t^2$ for $t \ll \tau$.

Let us finally note that from the point of view of interacting particles on a lattice we have studied the persistence dynamical susceptibility, instead of the density-density correlations discussed in the Introduction. This is because for the lattice gas problem at hand, the former does not show any interesting properties: except when a defect passes by, the local state is always the same—i.e., occupied. For completeness, we give the corresponding results in Appendix B 4. In a real system, however, the local configuration is going to be affected by the passage of a mobility defect, and one can expect that the density-density correlations will in fact

behave more like the persistence dynamical susceptibility computed before. The correspondence between persistence and self-intermediate scattering function is studied explicitly in kinetically constrained models in Ref. [52].

B. Kinetically constrained models: Numerical results

Kinetically constrained models (KCM's) postulate that glassy dynamics can be modeled by forgetting about static interactions between particles, putting all the emphasis on dynamical aspects. Among those models are, for example, the FA model or the Kob-Andersen (KA) model on hypercubic lattices [15,25]. The dynamics of these models can be understood in terms of diffusion of defects [17,21,25] and the models can be classified into cooperative and noncooperative models, depending on the properties of such defects. For cooperative models the size ξ_0, the density, and the time scale for motion of the defects depends on the particle density (for conservative models) or temperature (for nonconservative models) and change very rapidly with increasing density or decreasing temperature [25]. KA and FA models with more than one neighboring vacancy needed in order to allow the motion of other vacancies belong to this class. On the other hand, for the one-spin isotropically facilitated FA model, a single facilitating spin is a mobile defect at all values of temperature and the model is noncooperative. A recent analysis [21] suggests that for these models defects can be considered as noninteracting in $d>4$, while for $d<4$ the role of fluctuations becomes important. Therefore we expect that the previous results for the independent diffusing defects model should apply exactly for FA one-spin facilitated in $d>4$. Furthermore, since the corrections to the Gaussian exponents are not very large [21] in three dimensions, we still expect a semiquantitative agreement. In particular the initial increase of the dynamic susceptibility as $\chi_4(t)\sim N(t)^2$, where $N(t)$ is the total number of distinct visited sites, is expected to be quite a robust result. Also, we expect a diffusive growth of the dynamical length scale $\xi(t)$ governing the scaling of G_4, at least in the limit $\xi(t)\gg\xi_0$. At smaller times, one expects a crossover between a CRR regime when $Dt\ll\xi_0^2$ (where the dynamics inside the defects becomes relevant in cooperative models to a mobility defect regime for longer times). Hence, in principle, looking at the detailed properties of $G_4(r,t)$ one should be able to extract the defect properties—density, size, time scale—and decide which theoretical scenario is most consistent with numerical results.

In the following, we discuss numerical results for the one-spin-facilitated FA model both in $d=1$ and $d=3$ and for the $d=1$ East model where facilitation is anisotropic [15]. The two models can be described, respectively, in terms of diffusive and subdiffusive noncooperative defects and indeed the numerical results are in quantitative agreement with the predictions of the previous section, as will be explained in detail. We do not address the case of cooperative KCM models, for which a more complicated behavior is expected. Indeed a first slowing down of dynamics should occur near a dynamical crossover displaying the properties of an MCT-like avoided transition [25]. In this regime the model cannot be approximated as a system of independent freely diffusing defects and deriving a quantitative prediction for the behavior of four-point correlation and susceptibility would deserve further work. Such avoided transition should then be followed at lower temperature or higher density by an asymptotic behavior described in terms of cooperative diffusing defects.

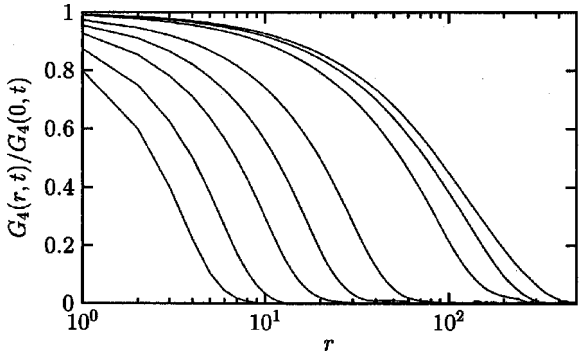

FIG. 2. Four-point spatial correlator (33) in the $d=1$ FA model at fixed temperature $T=0.2$ and various times $t=10^3,3\times10^3$, 10^4, $3\times10^4,10^5,10^6,3\times10^6,6\times10^6$ (from left to right). The correlator is normalized by its $r=0$ value. At this temperature, the relaxation time is $\tau\sim10^6$, so that time scales cover both regimes where t/τ is smaller and larger than 1.

1. One dimension

Let us start with the simplest model, the $d=1$ FA model. For a given temperature, we consider the time evolution of the following quantities. The analog of the spatial four-point correlator for this model is

$$G_4(r,t)=\frac{1}{N}\sum_{i=1}^{N}[\langle n_i(t)n_{i+r}(t)\rangle-n^2(t)], \tag{33}$$

where $n(t)=N^{-1}\Sigma_{i=1}^{N}\langle n_i(t)\rangle$ is the mean persistence, $n_i(t)$ being the persistence at site i. We also measure the corresponding four-point structure factor

$$S_4(k,t)=\frac{1}{N}\sum_{\ell,m=1}^{N}[\langle n_\ell(t)n_m(t)\rangle-n^2(t)]e^{ik\cdot(\ell-m)}, \tag{34}$$

and as usual we get the four-point susceptibility as the $k\to0$ limit of the structure factor, $\chi_4(t)=S_4(k=0,t)$. We generally find that the results are in good agreement with the free-defect model described above, at least at sufficiently low temperatures.

In Fig. 2, we show the evolution of the spatial correlator (33) at a given low temperature $T=0.2$ and various times. At this temperature, the relaxation time is about $\tau\sim10^6$, so that the time scales presented in Fig. 2 cover a range of times both smaller and larger than τ. The dynamic susceptibility $\chi_4(t)$ has the usual shape with a maximum at a time close to τ, indicating that dynamics is maximally heterogeneous there. This nonmonotonic behavior of χ_4 in fact does not show up in the spatial correlators of Fig. 2, which display instead a smooth monotonic evolution with time. The spatial decay of $G_4(r,t)$ becomes slower when t increases, indicat-

ing the presence of a monotonically growing dynamic length scale $\xi(t)$.

One can estimate the time dependence of $\xi(t)$ by collapsing the data of Fig. 2 using a form like

$$G_4(r,t) \sim G_4(0,t)\mathcal{G}\left(\frac{r}{\xi}\right). \tag{35}$$

Doing so, we find that $\xi \sim t^{0.45}$ is a reasonable representation of the data at $T=0.2$. Correspondingly, we find that the increase of $\chi_4(t)$ for $t<\tau$ is well described by a power law $\chi_4 \sim t^{0.85}$, so that the expected scaling $\chi_4 \sim \xi^2$ is reasonably verified given the unavoidable freedom in estimating the range of time scales where power laws apply. The values of these exponents are not far from the ones expected from freely diffusing defects in one dimension, although slightly smaller. Indeed, we recall that the results in Appendix B 1 predict $\xi=\sqrt{Dt}$, $\chi_4(t) \propto \rho\xi(t)^2$, and $\chi_4(t^*)=1/\rho$, where ρ is the density of defects, D their diffusion coefficient, and t^* the time at which $\chi_4(t)$ reaches its maximum value. This last prediction is also in good agreement with the numerical results (see, e.g., [20]).

Repeating the simulation at lower temperature $T=0.15$, we obtain $\chi_4 \sim t^{0.93}$, showing that deviations from theoretically expected values are partly due to preasymptotic effects that presumably disappear at very low temperatures.

It is important to remark that the scaling form (35) is only approximately supported by the data. The scaling in fact deteriorates when times become larger than τ. This can be seen in Fig. 2 where data for large times become more and more stretched, indicating an increasing polydispersity of the dynamical clusters. Note that a change in the shape of the spatial correlator makes a quantitative determination of ξ problematic. Usually, one wants to collapse various curves using a form like Eq. (35) to numerically extract ξ. Strictly speaking, this is not possible here if one works at fixed T and varying t over a large time window. This difficulty provides a second possible explanation for the small discrepancy between the measured values of exponents and the theoretical expectations.

The observation of a monotonically growing length begs the question: how can the correlation length increase monotonically with time while the volume integral of the spatial correlator χ_4 is nonmonotonic, as reported in the previous section? This is due to the fact that we have presented in Fig. 2 results for the normalized correlator $G_4(r,t)/G_4(r=0,t)$. By definition, $G_4(0,t)=n(1-n)$; hence, the normalization itself exhibits a nonmonotonic behavior. If one considers the normalized susceptibility $\tilde{\chi}_4=[G_4(0,t)N]^{-1}\Sigma_{\ell,m}[\langle n_\ell n_m\rangle - n^2(t)]$, one indeed finds that $\tilde{\chi}_4$ is monotonically growing as well.

In numerical works, the quantities that have been studied are in fact, most of the time, normalized, and the corresponding $\tilde{\chi}_4(t)$ observed for realistic systems shows a peak, at variance with what is observed in the $d=1$ FA model. As we shall show below, this is due to the one-dimensional nature of the model, and this difference is not observed in three dimensions. This difference in the behavior of the normalized dynamical susceptibility between one and three dimensions is indeed in full agreement with the independent defect diffusion computation; see the previous section and Appendix B.

Results are qualitatively similar in the one-dimensional East model. The dynamic susceptibility $\chi_4(t)$ develops a peak that grows and whose position is slaved to the increasing relaxation time when temperature decreases. At fixed temperature, a monotonically growing length scale is observed, while the scaling relation $\chi_4 \sim \xi^2$ still holds within our numerical precision. The novelty of this model lies in the fact that exponents are now temperature dependent, as all other dynamic exponents in this model. For instance, we find that $\xi(t) \sim t^{0.28}$ at $T=0.4$, $\xi(t) \sim t^{0.15}$ at $T=0.2$. These results are in agreement with the above predictions of the independent defect model if the defect motion is subdiffusive, with a dynamic exponent $z=T_0/T$, as expected from [17]. Due to the quasi-one-dimensional nature of the relaxation process in the three-dimensional generalization of the East model [18], these results most probably carry over to larger dimensions where they would differ by numerical factors only.

2. Three dimensions

In $d=3$, the situation is more subtle. Results for the normalized susceptibility of the one-spin-facilitated FA model were presented in Ref. [22], where it was found to have the standard nonmonotonic shape already described several times above. We find that the non-normalized $\chi_4(t)$ has the same qualitative behavior. Therefore, contrary to the $d=1$ case normalization is not a crucial issue in three dimensions.

In the following we check the predictions for independent diffusing defects in three dimensions for the susceptibility and correlation length obtained above—i.e., $\xi(t)=\sqrt{Dt}$, $\chi_4(t) \propto \rho\xi(t)^4$, and $\chi_4(t^*)=1/\rho$, where ρ is the density of defects, D their diffusion coefficient, and t^* the time at which $\chi_4(t)$ reaches its maximum value. We find a semiquantitative agreement with above prediction, with small deviations in the exponents that should be due to the interaction among defects. In particular the scaling of the peak with the density of defects was already analyzed in [22], where the result $\chi_4(t^*) \propto 1/\rho^{1-\epsilon}$ was obtained, with $\epsilon \simeq 0.03$. As for the correlation length, we find $\xi(t) \propto t^{0.42}$, which shows again a small deviation from the diffusive prediction. Regarding the increase at $t \ll \tau$ of the susceptibility we find a power law as predicted. As in $d=1$, the exponent changes slightly when decreasing temperature because the scaling regime where the power law applies becomes more and more extended. We find $\chi_4 \sim t^{1.4}$ at $T=0.25$, $\chi_4 \sim t^{1.55}$ at $T=0.17$, and $\chi_4 \sim t^{1.89}$ at $T=0.095$. This seems to indicate that the deviation from the scaling $\chi_4(t) \propto t^2$ calculated for the independent diffusing defect model is partly due to preasymptotic effects that are less and less important at lower temperature. Unfortunately, we were not able to measure ξ at much lower temperatures with sufficient accuracy. We expect that even at very low temperature a small deviation from the exponent of independent defects should survive due to the interaction among defects.

In Fig. 3 we show the four-point correlations in both real and Fourier space, Eqs. (33) and (34). In these curves the temperature is fixed at a low value, $T=0.17$, and time is

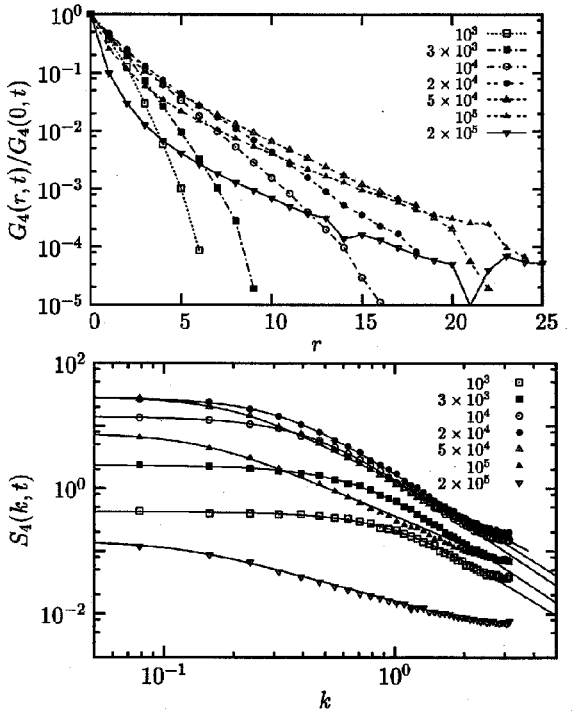

FIG. 3. Four-point correlations in the $d=3$ one-spin-facilitated FA model in both real space (left) and Fourier space (right) at fixed temperature $T=0.17$ and various times indicated in the figures. In Fourier space, points represent numerical data, while solid lines are fits to the form (36) with fitting parameters described in the text.

varied in a wide range that includes the relaxation time $\tau(T=0.17)\sim 5\times10^4$, where the dynamic susceptibility also peaks. For times $t\ll\tau$, the spatial decay of $G_4(r,t)$ is fast. When t increases, the spatial decay becomes slower, once again indicative of an increasing dynamic correlation length $\xi(t)$. When t becomes larger than τ, however, spatial correlations seem to become weaker. It is obvious from Fig. 3 that the volume integral of $G_4(r,t)/G_4(0,t)$ decreases when t grows larger than τ. This is very different from the one-dimensional case in Fig. 2, but consistent with all known numerical results.

However, a closer look at Fig. 3 reveals that even though the initial spatial decay of $G_4(r,t)$ is stronger at larger times, the contrary is true at large distances. This indicates that the topology of the dynamic clusters changes when t grows larger than τ, but that $\xi(t)$ may keep increasing in a monotonic manner. Since the spatial correlator is very small at large distances, quantitative measurements of $\xi(t)$ are more easily performed in Fourier space via $S_4(k,t)$.

At short time, a fit of $S_4(k,t)$ using the functional form given by Eq. (31) works reasonably well, but the fit quickly deteriorates at long time. We have therefore used the following generalization of Eq. (31):

$$S_4(k,t)=\chi_4(t)\mathcal{F}_\beta[k^2\xi^2(t)],\quad \mathcal{F}_\beta(u)\equiv\frac{2^{2/\beta}}{u^\beta}(u-1+e^{-u})^{\beta/2}. \tag{36}$$

Freely diffusing defects correspond to $\beta=2$ and $\xi(t)\sim\sqrt{t}$. Using $\beta(t)$ as an additional free parameter, we are able to fit $S_4(k,t)$ at all times; see Fig. 3. We find that β decreases from $\beta\approx2.5$ at small times to $\beta\approx1$ for the longest time scales investigated, which corresponds to $t\approx5\tau$. At such large times, the dynamic susceptibility has already decreased by a factor of ≈300 from its maximum value at $t=\tau$, and correlations become very weak indeed. The values for β found from the fits are consistent with the value $\beta\approx2.15$ reported in Ref. [22] where only fixed time ratio $t/\tau(T)=1$ at different temperatures have been studied. From this fitting procedure, we deduce a monotonically growing dynamic length $\xi(t)$, even beyond $t=\tau(T)$. Fitting its time dependence with a power law, we get $\xi\sim t^{0.42}$ which appears to be slightly subdiffusive, but close to the value found above in the one-dimensional case.

In conclusion we find that on small enough time scales, one indeed has good agreement with the above calculations based on freely diffusing defects; therefore, defect branching and defect coagulation can be neglected. However, for longer time scales, significant deviations appear which correspond to the evolution of the exponent $\beta(t)$ and should be responsible for the small deviations of the predicted exponent for χ_4. Physically, the time evolution of the exponent $\beta(t)$ characterizing the large-k behavior of the dynamic structure factor is reasonable. At very short times, dynamic clusters consist of coils created by random walkers, and an exponent close to $\beta=2$ can be expected. For times $t\sim\tau$, clusters look critical, as described in Refs. [21,22], and the exponent $\beta=2-\eta$, $\eta<0$ is expected. At very large times, clusters are most probably extremely polydisperse because the remaining spatial correlations at large times are due to the largest regions of space that were devoid of defects at time 0 and that take therefore a large time to relax. But at large times, some isolated sites that have not been visited by defects during the relaxation might survive so that the distribution of dynamic clusters at large times is very wide; see Ref. [18] for snapshots. A small value of β can therefore be expected.

VII. NUMERICAL RESULTS ON ATOMISTIC MODEL SYSTEMS

In this section, we study numerical results for the dynamic susceptibility and structure factor of a supercooled liquid simulated by molecular dynamics simulations. The model we study is mainly the well-known binary Lennard-Jones (LJ) mixture as first defined and studied in Ref. [53], but we report also some results for a soft-sphere mixture studied in [38,55,56]. We do not give details about our numerical procedures since these were given several times in the literature [21,30,53].

A. Dynamical susceptibility

In previous works on various realistic liquids, the dynamic susceptibility was reported several times [9,10,12,28]. It is known to exhibit at peak at a time scale enslaved to the quantity chosen to quantify local dynamics. Typically, particle displacements are chosen, and one computes therefore the variance of some dynamical correlation,

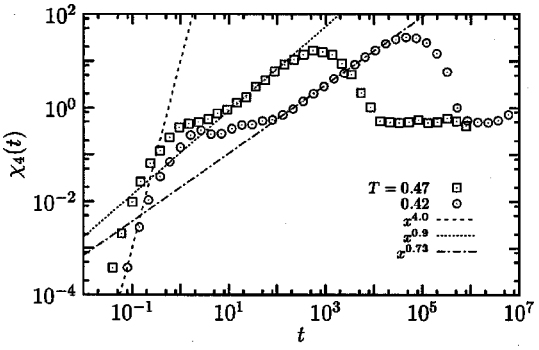

FIG. 4. Time dependence of the dynamic susceptibility in the binary LJ mixture at two different temperatures (imposed using a ''velocity rescaling'' thermostat). The lines are power-law fits with exponents indicated in the label.

$$\chi_4(t) = N[\langle F^2(t)\rangle - \langle F(t)\rangle^2], \tag{37}$$

with

$$F(t) = \frac{1}{N}\sum_{i=1}^{N} F_i(t). \tag{38}$$

The dynamic quantity $F_i(t)$ can be chosen as some "persistence" function, in which case $\langle F(t)\rangle$ resembles the overlap function usually measured in spin systems [10,12,28]. Other choices are [21,30]

$$F_i(t) = \cos[\vec{q}\cdot\delta\vec{r}_i(t)], \tag{39}$$

where $\vec{q}$ is a wave vector chosen in the first Brillouin zone and $\delta\vec{r}_i(t)$ is the displacement of particle i in a time interval t. In the limit of small $|\vec{k}|$, it is better to study $F_i(t) = |\delta\vec{r}_i(t)|/\sqrt{\Delta r^2(t)}$, where $\Delta r^2(t)$ is the mean-square displacement of the particles [9,11].

Whereas the general shape of $\chi_4(t)$ is well documented in the literature, its precise time dependence was never discussed. In Fig. 4, we present the time dependence of $\chi_4(t)$ in the binary Lennard-Jones mixture at two different temperatures. The data are presented in a log-log scale, in order to emphasize the existence of several time regimes that are generally hidden in the existing reports. To build these curves, we choose Eq. (39) as the local observable, for a wave vector that corresponds roughly to the typical interparticle distance.

In the ballistic regime at very short times, we find that $\chi_4(t) \sim t^4$, as described in Sec. II. The system then enters the time regime where dynamic structure factors typically exhibit plateaus, as a result of particle caging. As seen in Fig. 4, this is also the case for $\chi_4(t)$. Finally, $\chi_4(t)$ reaches a maximum located close to the relaxation time extracted from the time dependence of $\langle F(t)\rangle$ and then rapidly decays to its long-time limit, equal to $1/2$ in the present case. In Fig. 4, we fitted the time dependence of the increase of $\chi_4(t)$ towards its maximum with power law $\chi_4 \sim t^{\mu}$. The fits are satisfactory, although they only hold on restricted time windows. We find a slight temperature dependence of the exponent μ. For instance, we find $\mu \approx 0.9$ at $T=0.47$ and $\mu \approx 0.73$ at $T=0.42$. As already discussed in the case of kinetically constrained models above, it is not clear how the restricted time window used to determine the exponents might affect their values. However, the data in the Lennard-Jones system behave quantitatively very differently from both theoretical results obtained from freely diffusing defects and numerical results in the one-spin-facilitated $d=3$ FA model, where $\mu=2$. The small temperature evolution in the LJ liquid differs even qualitatively from the one-spin-facilitated $d=3$ FA model where the exponent was found to increase when decreasing temperature. These observations tend to discard a description of this supercooled liquid via a scenario with simple independently diffusing defects, even interacting ones. The above value of μ is in principle compatible with the predictions of elasticity theory, which yields $\mu=1/2$ or $\mu=1$ depending on the damping of phonons. However, the time scale in which the above-mentioned power-law behavior holds in the Lennard-Jones mixture corresponds to the β regime where the displacement of particles is no longer small and the elastic description unjustified. Within MCT, on the other hand, χ_4 should increase in that regime with an exponent $\mu=b$ that is known from previous analysis, $b \approx 0.63$ [54]. The values found above are somewhat larger, but it is hard to know how preasymptotic effects influence the numerical data. Moreover, the value closest to b, $\mu \approx 0.73$, is obtained for $T=0.42$, a temperature already lower than the mode-coupling singularity located at $T_c \approx 0.435$ in this system (a linear interpolation between the values at $T=0.47$ and $T=0.42$ gives $\mu \approx 0.78$ at $T=0.435$). MCT also provides a prediction for the height of the peak, $\chi_4^* \sim t^{*1/\gamma}$, where γ was predicted to be ≈ 2.3, leading to $\lambda = 1/\gamma \approx 0.43$. This prediction is in good agreement with the results of Ref. [21] where $\chi_4(t^*) \sim t^{*0.4}$ was reported. It is important to remark, however, that the MCT exponents are not very well determined. The exponents we reported are the ones computed theoretically in [54]. The exponents obtained from the fits of the numerical data based on MCT are a bit different [53], in particular $b \approx 0.5$ and $1/\gamma \approx 0.37$.

If one insists on using a noncooperative kinetically constrained model to describe the Lennard-Jones liquid, the small value of the short time exponent μ forces one to choose a "fragile" KCM model, such as the East model described above, where the exponent for the dynamic susceptibility is found to be much smaller than the diffusive value $\mu=2$, and indeed to decrease when temperature is decreased. On the other hand, the large dynamic length scales observed in the Lennard-Jones system are not expected for fragile KCM's such as the East model [18]. Our results do not discard the possibility that cooperative KCM's (in a proper density or temperature regime) display a four-point correlation and susceptibility quantitatively similar to the one of the Lennard-Jones liquid. Indeed, as stressed, in e.g., [25], for these models one expects a first regime of slowing down of dynamics due to an avoided mode-coupling transition. The susceptibility and four-point correlation could then well be quantitatively comparable to that of Lennard-Jones liquids. Concerning these comparisons between theoretical scenarios and molecular dynamics simulation results it is important to notice that the the relevance of supposedly "fragile" numerical models for supercooled liquids in shedding light on real fragile glass formers has been questioned [57].

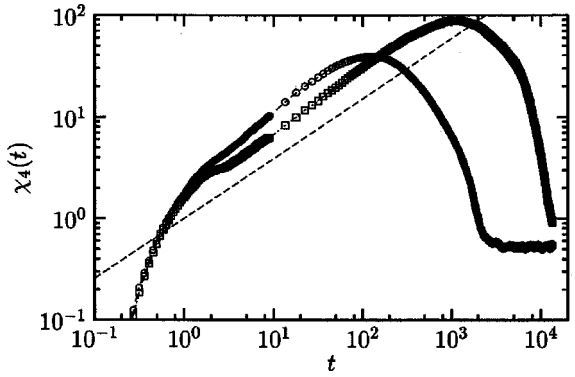

FIG. 5. Dynamic susceptibility $\chi_4(t)$ at $T=0.3$ and 0.26 (from left to right) in a log-log plot as a function of time for the soft-sphere binary mixture of Refs. [38,56]. The data were kindly provided to us by D. Reichman and R. A. Denny, who worked in the NVE ensemble. The straight line represents the MCT prediction for the power-law behavior before the peak.

Finally, it is of course a natural question to ask whether the above agreement between MCT predictions and numerical results is only restricted to the Lennard-Jones system. Using the unpublished data of Ref. [56] for a soft-sphere binary mixture where $T_c \simeq 0.22-0.24$ [38,55] we actually found very similar results. Close to T_c a power-law behavior of χ_4 as a function of time can again be observed. For instance, $\chi_4 \sim t^{0.63}$ for $T=0.26$. In Fig. 5 we plot χ_4, defined as in Ref. [28], as a function of time. We also display the power-law behavior predicted by MCT before the peak with the exponent $b \simeq 0.59$ taken from Ref. [55]. There is a similar agreement between the exponent λ measured from the height of the peak and the value of $1/\gamma$ extracted from an MCT analysis of the data. (As in the previous case we used the theoretical MCT exponents computed in [55]. In the case of the soft-sphere system the MCT exponents from numerical fits have probably a large error bars; see the discussion in [54].)

The fact that the predictions of MCT for the four-point susceptibility are in reasonable agreement with numerical simulations in both systems is significant, since the exponents b and $1/\gamma$ are measured on (local) two-point functions and μ and λ on four-point functions. The relation between these exponents test a rather deep structural prediction of MCT that relates time scales to length scales [32]. More numerical work, on other model systems with different values of b, for example, would be needed to establish more firmly whether the coincidence observed in the present paper is or not accidental.

B. Growing length scale?

We focus now more directly on the dynamic length scale. In previous works, the dynamic length scale ξ extracted from four-point correlations was measured either at fixed temperature for various times t where it was found to be nonmonotonic [12,13,27], but monotonic in [11], or at fixed time $t=\tau(T)$, for different temperatures, where it is found to be increasing when the temperature decreases [9,12,21]. In practice, to extract $\xi(t,T)$ from the four-point correlation function either in real space or in Fourier space, one needs to postulate a specific functional form of G_4. In this respect, the results of the previous section on simple lattice KCM's with no underlying liquid structure prove instructive. It is clear that with data similar to Fig. 3, but obtained with much smaller system sizes, with much less statistics, and polluted by the underlying structure of the liquid, the precise extraction of dynamical length scales from molecular dynamics simulations is not an easy task. More fundamentally, extracting ξ from fitting either $G_4(r,t)$ or $S_4(k,t)$ to a time-independent scaling form necessarily biases the data as discussed above. This also shows that it is a much easier and safer procedure to work, say, at $t=\tau(T)$ and different temperature to observe the growth of a cooperative length $\xi(\tau,T)$ when decreasing T. On the other hand, it is not *a priori* granted that the growth law of ξ with $t=\tau(T)$ when changing T is identical to that of $\xi(t,T)$ with t at a given temperature T. We will not be able to answer this question with our numerical data.

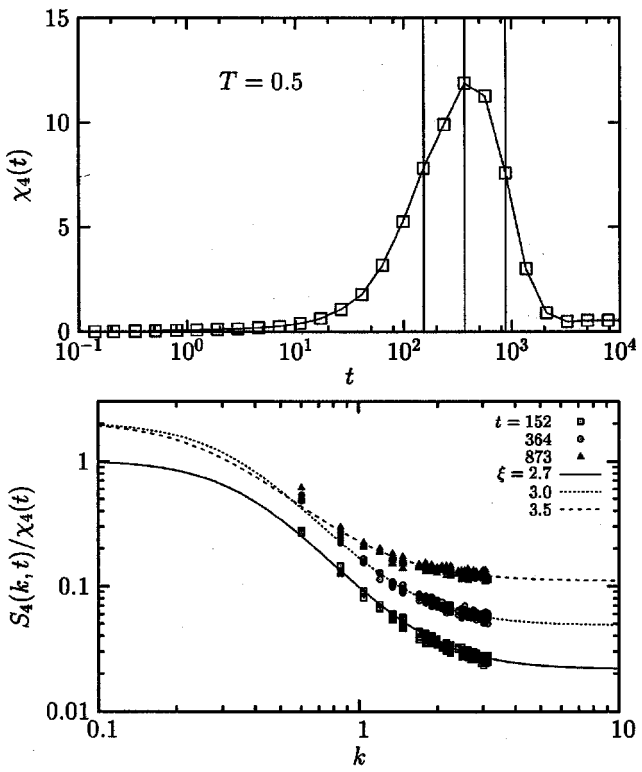

FIG. 6. Left: dynamic susceptibility at $T=0.5$ and $q=4.21$. The vertical lines indicate the times at which $S_4(k,t)$ is evaluated in the bottom figure. Right: the corresponding three $S_4(k,t)$ (the last two have been multiplied by 2 for clarity). Lines are fits to the form (40), the $k \to 0$ limit being fixed by the value of $\chi_4(t)$, with a monotonically growing length scale $\xi(t)$.

With the above caveats in mind, we present in Fig. 6 some numerical data in the binary Lennard-Jones mixture at a fixed temperature $T=0.5$ and three different times which fall before, at, and after the peak in $\chi_4(t)$. The difficulty of getting clear-cut quantitative determinations for ξ is obvious from Fig. 6. One would need much larger system sizes to properly measure $S_4(k,t)$ at small wave vectors, large times,

and low temperatures. The system simulated here contains 1372 particles. One could possibly increase the number of particles by a factor of 10, but the increase in linear size would be very modest, a factor of $10^{1/3} \approx 2.15$. Nonetheless, we have fitted the data in Fig. 6 with a simple empirical form

$$S_4(k,t) = \frac{\chi_4(t) - C}{1 + (k\xi)^\beta} + C \tag{40}$$

for $0 \leqslant k < k_0$, $k_0 \approx 7.21$ being the position of the first peak in the static structure factor. As for the $d=3$ FA model, the exponent $\beta(t)$ and the dynamic length $\xi(t)$ are fitting parameters. There is an additional free parameter, the additive constant C in Eq. (40), which accounts for the fact that the structure of the liquid starts to be visible and creates some signal in $S_4(k,t)$ when $k \to k_0$. The results of the fitting procedure are presented in Fig. 6 with lines going through the data. Note that the fits in Fig. 6 are constrained at low k by the value of the dynamic susceptibility $\chi_4(t)$. The most important result from Fig. 6 is that if the functional form of $S_4(k,t)$ is given some freedom, here via the time-dependent exponent $\beta(t)$, the extracted dynamic length scale $\xi(t)$ indeed continues to grow monotonically after the peak of the dynamic susceptibility, contrary to reported previously [12,13,27], but in agreement with [11]. We emphasize once more that this result physically makes sense. At times much larger than t^*, only very rare but very large dynamical domains contribute to the dynamic structure factor, so that spatial correlations are weak, but extremely long ranged. The existence of an ever growing length scale is supported by any model with an hydrodynamical limit (such as the phonon or defect models studied here) and is in a sense trivial. The really interesting piece of information is the value of this length scale for $t = \tau_\alpha$—i.e., when the relevant relaxation processes take place.

We conclude that our numerical data are not inconsistent with a monotonically growing length scale even for $t > \tau$, although addressing more quantitative issues such as functional form at the growth law and its temperature dependence would require quite an important, but certainly worthwhile, numerical effort.

VIII. CONCLUSION AND FINAL COMMENTS

Let us summarize the results and various points made in this rather dense paper. First, we have computed numerically and analytically, exactly or approximatively, the four-point correlation function designed to characterize nontrivial cooperative dynamics in glassy systems within several theoretical models: mode-coupling theory, collectively rearranging regions, diffusing defects, kinetically constrained models, and elastic and plastic deformations. The conclusion is that the behavior of $\chi_4(t)$ is rather rich, with different regimes summarized in the Introduction and in Fig. 1. We have computed the early time exponent μ and the peak exponent λ for quite a few different models of glass-forming liquids and shown that the values of these exponents resulting from these models are quite different, suggesting that the detailed study of $\chi_4(t,T)$ should allow one to eliminate or confirm some of the theoretical models for glass formation.

In this spirit, we first simulated some noncooperative KCM's as the one-spin-facilitated FA model in $d=1$ and $d=3$ and the East model. The assumption of pointlike defects that diffuse, possibly with an anomalous diffusion exponent, gives a good account of the shape of the four-point correlation function and of the four-point susceptibility which are in quantitative agreement with the above results for the independent defect model. For strong glasses such as SiO_2, our results might lead to quantitative predictions if the relaxation is indeed due to defect diffusion. It would be very interesting to reconsider numerical simulations of the dynamics of SiO_2 under the light of the present paper to check in more detail that the defect picture is indeed correct in this case (note that our results should enable one to extract, in principle, the properties, density, and relaxation times of defects from the four-point correlation function). For the $d=3$ one-spin-facilitated FA model, we see clear indications of the interactions between defects as time increases. This leads to small deviations of the numerically obtained exponents with respect to those predicted by our analysis of the independent defect model, which does not account for interactions between defects. As far as the identification of a growing length scale $\xi(t)$ from numerical data, we have seen that even within this simplified lattice model, this can be a rather difficult task. Our results point toward a dynamical correlation length that grows forever and a behavior of $S_4(k,t)$ different from the Ornstein-Zernike form but with similar asymptotic behavior. We leave the study of cooperative KCM's, for which a more complicated behavior should occur, for future work. In particular, the detailed form of $S_4(k,t)$ should contain information about the inner structure of the corresponding defects.

We have also analyzed the four-point susceptibility of both a Lennard-Jones system and a soft-sphere system, and shown that the initial exponent μ of the four-point susceptibility is decreasing with the temperature and rather small, $\mu < 1$. We have found, perhaps unexpectedly, a reasonable agreement for μ and λ with the predictions of MCT but not with other theoretical scenarios, such as simple diffusive or subdiffusive defects, strong KCM's, or CRR's (although this might be a question of temperature and time scales, since both CRR and cooperative KCM's are supposed to apply closer to the glass transition temperature). Finally we confirm that the extraction of the growth law of $\xi(t)$ at a given temperature is difficult, and we can only say at this stage that the data are not incompatible with the idea that $\xi(t)$ grows monotonically, even beyond $t = \tau_\alpha$, in the Lennard-Jones system.

As for further work and perspectives, we think that the following points would be worth investigating. First, it would be very interesting to develop a detailed theory of the crossover between the elastic regime described in Sec. III and the mode-coupling β relaxation regime. Is it possible, in particular, to describe approximately the "melting" of the glass as one approaches the mode-coupling transition temperature from below? Second, we only considered systems in equilibrium. One in fact expects that the four-point susceptibility also contains very useful information in the aging regime (see [31,59]). Detailed predictions in this regime may

enable one to probe the mechanisms for slow dynamics and the issue of the cooperative length at low temperature in the aging regime [59]. In particular, the elastic contribution should not age whereas the CRR contribution (characterized by the same exponent μ) should exhibit some aging, possibly allowing one to separate the two effects. Third, since it is clear from the present paper that simpler KCM's (Fredrickson-Andersen one-spin-facilitated, East model and its generalization) seem to fail at describing quantitatively $\chi_4(t)$ obtained by molecular dynamics simulations of (at least two) fragile systems, it would be important to understand if it is possible to find a generalization of these KCM's that can be in agreement with numerics. For the same reason a quantitative study of four-point functions in cooperative KCM's where defects have a complex inner structure would be interesting. Fourth, it would be important to define more complicated correlation functions—for example, a fully general four point function or higher-order correlation functions—in order to test in a more stringent way the idea of cooperativity in glassy systems and distinguish systems where the growth of $\chi_4(t)$ is trivial, such as elastic solids, from those in which a truly nontrivial cooperativity governs the dynamics. Finally, it seems clear that this issue of cooperativity and its associated length scale can only be convincingly settled if long-time scales and low-temperature regimes can be probed quantitatively in experimental systems. We hope that the present paper will motivate ways to directly access four-point functions experimentally in glassy systems (see [31]); natural candidates for this are colloids [3] and granular materials [58,60], although there might be ways to investigate this question in molecular glasses and spin glasses as well [61].

Note added to proofs: We have recently realized that the dynamical susceptibility can be quite different in the canonical NVT ensemble and in the NVE ensemble. A full discussion of this point, and its consequences for the analysis of numerical and experimental results, will be presented in [45].

ACKNOWLEDGMENTS

Figure 5 was obtained from the unpublished data of D. R. Reichman and R. A. Denny. We are very grateful to them for providing these results. We thank E. Bertin, D. Chandler, O. Dauchot, J. P. Garrahan, A. Pan, and D. R. Reichman for discussions. G.B. is partially supported by the European Community's Human Potential Programme Contract No. HPRN-CT-2002-00307 (DYGLAGEMEM). C.T. is supported by the European Community's Human Potential Programme Contract No. HPRN-CT-2002-00319 (STIPCO).

APPENDIX A: DYNAMICS OF ELASTIC NETWORKS

1. Four-point correlation function: Overdamped case

We will define $G_4(\vec{r},t)$ for the elastic model defined in the text as

$$G_4(\vec{r},t) = \langle \cos q[\phi(\vec{r},t) - \phi(\vec{r},0)] \times \cos q[\phi(\vec{r}=0,t) - \phi(\vec{r}=0,0)]\rangle - C^2(q,t), \tag{A1}$$

which is equivalent to

$$G_4(\vec{r},t) = \frac{1}{2}\langle \cos q[\phi(\vec{r},t) - \phi(\vec{r},0) + \phi(\vec{r}=0,t) - \phi(\vec{r}=0,0)]\rangle + \frac{1}{2}\langle \cos q[\phi(\vec{r},t) - \phi(\vec{r},0) - \phi(\vec{r}=0,t) + \phi(\vec{r}=0,0)]\rangle - C^2(q,t).$$

Using the fact that the field ϕ is Gaussian, we finally find

$$G_4(\vec{r},t) = C^2(q,t)\{\cosh[2q^2R(\vec{r},t)] - 1\}, \tag{A2}$$

where

$$R(\vec{r},t) = \langle [\phi(\vec{r},t) - \phi(\vec{r},0)][\phi(\vec{r}=0,t) - \phi(\vec{r}=0,0)]\rangle = \frac{T}{\kappa}\int \frac{d^dk}{(2\pi)^d k^2} e^{-i\vec{k}\cdot\vec{r}}(1 - e^{-\kappa k^2 t}). \tag{A3}$$

Hence,

$$R(\vec{r},t) = \frac{T}{\kappa}(\kappa t)^{1-d/2} F\left(\frac{r}{\sqrt{\kappa t}}\right), \tag{A4}$$

with

$$F(z) = z^{2-d}[I(\infty) - I(z)], \quad I(z) = \int \frac{d^dw}{(2\pi)^d w^2} e^{-iw_1 - w^2/z^2}. \tag{A5}$$

We thus see immediately that $G_4(\vec{r},t)$ will be governed by a "diffusive" correlation length $\xi(t) \sim \sqrt{\kappa t}$, as expected from the structure of the Langevin equation that describes relaxational dynamics. Note that for underdamped dynamics, sound waves would change this scaling.

It is useful to consider the following quantity:

$$J(z) = \frac{\partial I(z)}{\partial\left(\frac{1}{z^2}\right)} = \int \frac{d^dw}{(2\pi)^d} e^{-iw_1 - w^2/z^2}. \tag{A6}$$

In $d=3$, after integrating over dw_1, one has

$$J(z) = \frac{1}{8\pi^{3/2}} z^3 e^{-z^2/4} \tag{A7}$$

and

$$I(z) = \frac{1}{4\pi^{3/2}} \int_z^\infty e^{-u^2/4} du. \tag{A8}$$

Therefore, for $z \ll 1$, one finds $F(z) \simeq (4\pi z)^{-1}$ and $R(\vec{r},t) \simeq T/(4\pi\kappa r)$, whereas for $z \gg 1$,

$$F(z) \simeq (2\pi^{3/2})^{-1} \exp(-z^2/4)/z^2.$$

Thus, for $r \ll \xi(t)$ and $\kappa\Lambda^2 t \gg 1$, the four-point correlation function behaves as

$$G_4(\vec{r},t) = f_q^2\left[\cosh\left(\frac{Tq^2}{2\pi\kappa r}\right) - 1\right]. \tag{A9}$$

2. Four-point correlation function: Underdamped case

We have now

$$m\frac{\partial^2\phi(\vec{r},t)}{\partial^2 t} = \kappa\Delta\phi(\vec{r},t), \tag{A10}$$

which has for solutions in Fourier space

$$\phi_k(t) = \exp(ikVt)\phi_k(0), \tag{A11}$$

with $V=(\kappa/m)^{1/2}$. We now have

$$\langle[\phi(\vec{r},t)-\phi(\vec{r},0)]^2\rangle = \frac{2T}{\kappa}\int\frac{|\exp(ikVt)-1|^2}{k^2}\frac{d^dk}{(2\pi)^d} = \frac{4T}{\kappa}\int(1-\cos[Vkt])dk. \tag{A12}$$

In $d=3$, we find obviously the same result for f_q and G_4 as above, but $R(\vec{r},t)$ is now equal to

$$R(\vec{r},t) = \frac{T}{\kappa}\int\frac{d^dk}{(2\pi)^dk^2}e^{-i\vec{k}\cdot\vec{r}}[1-\cos(kVt)], \tag{A13}$$

which we write

$$R(\vec{r},t) = \frac{T}{\kappa}[I(\vec{r},0)-I(\vec{r},t)], \tag{A14}$$

where

$$I(\vec{r},t) = \int\frac{d^dk}{(2\pi)^dk^2}e^{-i\vec{k}\cdot\vec{r}}\cos(kVt). \tag{A15}$$

By introducing $z=Vt/r$ and changing the variable $q\equiv rk$ and also $u=\cos\theta$ and integrating over u, one finds

$$I(\vec{r},t) = \frac{2\pi}{r}\int dqq^{-1}\{\sin[q(1+z)]+\sin[q(1-z)]\}. \tag{A16}$$

Consider the first term

$$I(\vec{r},t) = \frac{2\pi}{r}\int dqq^{-1}\sin[q(1+z)]. \tag{A17}$$

Changing variable $v=q(1+z)$ directly shows that this integral do not depend on z, as long as $(1+z)$ is positive. This is true for the other integral, which does not depend on z as long as $1-z$ is positive. If $1-z$ is negative, then the integral changes sign. Therefore we have that $I(\vec{r},t)=I(\vec{r},0)$ if $z<1$ and $I(\vec{r},t)=0$ if $z>1$. Therefore $R(\vec{r},t)=0$ if $z<1$ and $R(\vec{r},t)=T/4\pi\kappa r$ when $z>1$. The result is very intuitive: when $z<1$ the information does not have time to travel the distance r and there are no correlation. For $z>1$ the two regions are "connected" and one finds the free-field correlations. Brownian and Newtownian dynamics furnish the same correlation for a given r when the time diverges, as we expect. Finally, it is straightforward to obtain the result quoted in the text for $\chi_4(t)$.

3. Low-dimensional case

We give here, without much detail, the results for elastic networks in $d=1$ and $d=2$. In $d=1$, as is well known, each particle wanders arbitrary far from its initial position but in an anomalous, subdiffusing way, as $t^{1/4}$. Correspondingly, the dynamical structure factor decays as a stretched exponential:

$$\ln C(q,t) \sim \frac{T}{\kappa}q^2t^{1/2}. \tag{A18}$$

Note that the $t^{1/4}$ comes from a collective displacement of the cages and is similar to the anomalous diffusion observed for hard spheres in one dimension, since the latter problem can be mapped onto the Edwards-Wilkinson problem in one dimension [60,62]. We expect that the results obtained here for G_4 should also hold for this case as well. In fact, this model was recently discussed in the context of a simple $d=1$ granular compaction model, see [60].

In $d=2$, the displacement grows logarithmically with time, leading to a power-law decay of the dynamical structure factor with a q-dependent exponent:

$$C(q,t) \sim t^{-y}, \quad y = \frac{q^2T}{8\pi\kappa}. \tag{A19}$$

Turning now to $\chi_4(t)$, we find that after a short transient, $\chi_4(t)$ grows as $t^{1/2}$ in $d=1$ and behaves as t^{1-2y} in $d=2$.

APPENDIX B: CALCULATIONS FOR THE DEFECT MODEL

In Sec. VI we have reduced the computation of $G_4(r,t)$ and $\chi_4(t)$ to probability distributions of a single random walk. In the following we shall show how these quantities can be computed in any spatial dimension.

Let us call $F_x^z(u)$ be the probability that a random walk starting in z reaches x for the first time at time u. $P_x^z(t)$, the probability that a vacancy starts in z at time zero and reaches for the first time x at a time less than t, reads

$$P_x^z(t) = \int_0^t F_x^z(u)du. \tag{B1}$$

Therefore, we need to calculate $F_x^z(u)$. The trick to do that is writing a linear equation relating F_x^z, which we want to compute, to $P^z(x,t)$, the probability that a random walk with self-diffusion coefficient D, starting in z, is in x at time t, which is well known. This linear equation is

$$P^z(x,t) = \delta_{x,z}\delta_{t,0} + \int_0^t F_x^z(u)P^x(x,t-u)du. \tag{B2}$$

By taking the Laplace transform (from now on s is the variable conjugated to t and $\mathcal{L}$ indicates the Laplace transform) we obtain

$$F_x^z(t) = \mathcal{L}^{-1}\left(\frac{\mathcal{L}P^z(x,s)-\delta_{x,z}}{\mathcal{L}P^x(x,s)}\right)(t) \tag{B3}$$

and

$$P_x^z(t) = \int_0^t\mathcal{L}^{-1}\left(\frac{\mathcal{L}P^z(x,s)-\delta_{x,z}}{\mathcal{L}P^x(x,s)}\right)(t')dt' \tag{B4}$$

$$= \mathcal{L}^{-1}\frac{1}{s}\frac{\mathcal{L}P^z(x,s)-\delta_{x,z}}{\mathcal{L}P^x(x,s)}. \tag{B5}$$

A similar strategy can be used to calculate $P^z_{x,\bar{y}}(t)$. Indeed the following equality holds:

$$P^z_{x,\bar{y}}(t) = \int_0^t F^z_{x,\bar{y}}(t')P^x_{\bar{y}}(t-t')dt',$$

$$P^z_{y,\bar{x}}(t) = \int_0^t F^z_{\bar{x},y}(t')P^y_{\bar{x}}(t-t')dt', \tag{B6}$$

where $F^z_{\bar{x},y}(t)$ is the probability that a random walk starting in z at time zero reaches y for the first time at t but never touches x at $s \leqslant t$. Therefore, in order to calculate $P^z_{x,\bar{y}}(t) + P^z_{y,\bar{x}}(t)$ we need to calculate $F^z_{x,\bar{y}}(t) + F^z_{y,\bar{x}}(t)$. It is immediate to check that the following equations hold for any choice of x,z,y:

$$F^z_x(t) = \delta_{x,z}\delta_{t,0} + \int_0^t dsF^z_{\bar{x},y}(s)F^y_x(t-s) + F^z_{x,\bar{y}}(t),$$

$$F^z_y(t) = \delta_{y,z}\delta_{t,0} + \int_0^t dsF^z_{x,\bar{y}}(s)F^x_y(t-s) + F^z_{\bar{x},y}(t), \tag{B7}$$

which implies, again by Laplace transform (z is always different from x and y in the following so we will skip the Kronecker δ's),

$$F^z_{\bar{x},y}(t) + F^z_{x,\bar{y}}(t) = \mathcal{L}^{-1}\frac{\mathcal{L}F^z_x(s) + \mathcal{L}F^z_y(s)}{\mathcal{L}F^x_y(s) + \mathcal{L}F^x_x(s)}. \tag{B8}$$

Using the expression (B3) for $F^x_y(s)$ we get

$$F^z_{\bar{x}}(y,t) + F^z_{\bar{y}}(x,t) = \mathcal{L}^{-1}\frac{\mathcal{L}P^z(x,s) + \mathcal{L}P^z(y,s)}{\mathcal{L}P^x(y,s) + \mathcal{L}P^x(x,s)}. \tag{B9}$$

Furthermore, $P^y_{\bar{x}}(t) = 1 - P^y_x(t)$. Hence we obtain

$$\mathcal{L}P^y_{\bar{x}}(s) = \frac{1}{s} - \mathcal{L}P^y_x(s) = \frac{1}{s}\left(1 - \frac{\mathcal{L}P^y(x,s)}{\mathcal{L}P^x(x,s)}\right). \tag{B10}$$

Finally, we obtain the expression for

$$\mathcal{L}[P^z_{x,\bar{y}}(s) + P^z_{y,\bar{x}}(s)] = \frac{\mathcal{L}P^z(x,s) + \mathcal{L}P^z(y,s)}{\mathcal{L}P^x(y,s) + \mathcal{L}P^x(x,s)}\frac{1}{s}\left(1 - \frac{\mathcal{L}P^y(x,s)}{\mathcal{L}P^x(x,s)}\right). \tag{B11}$$

A useful way to rewrite this expression is obtained by summing and subtracting the Laplace transform of $P^z_x(t) + P^z_y(t)$:

$$P^z_{x,\bar{y}}(t) + P^z_{y,\bar{x}}(t) = P^z_x(t) + P^z_y(t) - 2\mathcal{L}^{-1}\frac{\mathcal{L}P^z(x,s) + \mathcal{L}P^z(y,s)}{\mathcal{L}P^x(y,s) + \mathcal{L}P^x(x,s)}\frac{1}{s}\frac{\mathcal{L}P^y(x,s)}{\mathcal{L}P^x(x,s)}. \tag{B12}$$

Finally putting together all the different terms we have

$$\langle n_x(t)n_y(t)\rangle = \exp[-2\rho_v - 2\rho_v N(t) + 2\rho_v P^y_x(t) + \rho_v G(t,x-y)], \tag{B13}$$

where $N(t) = \Sigma_{z\neq x}P^z_x(t)$ is the average number of distinct sites (minus 1) visited by a random walk during the interval of time t and

$$G(t,x-y) = \mathcal{L}^{-1}\left[\sum_{z\neq x,y}\frac{\mathcal{L}P^z(x,s) + \mathcal{L}P^z(y,s)}{\mathcal{L}P^x(y,s) + \mathcal{L}P^x(x,s)}\frac{1}{s}\frac{\mathcal{L}P^y(x,s)}{\mathcal{L}P^x(x,s)}\right]. \tag{B14}$$

Since

$$\langle n_x(t)\rangle^2 = \exp[-2\rho_v - 2\rho_v N(t)], \tag{B15}$$

the expression of G_4 is

$$G_4(x-y,t) = \exp[-2\rho_v - 2\rho_v N(t)] \times\{\exp[2\rho_v P^y_x(t) + \rho_v G(t,x-y)] - 1\}. \tag{B16}$$

In the following we shall analyze separately the one-dimensional case, the three- or higher-dimensional case, and the two-dimensional case.

1. One dimension

Consider a symmetric random walk on a one-dimensional lattice with lattice spacing a. By Laplace transforming the master equation

$$\frac{dP^z(x,t)}{dt} = \frac{P^z(x+a,t) + P^z(x-a,t) - 2P^z(x,t)}{2}, \tag{B17}$$

one immediately obtains

$$\mathcal{L}P^z(x,s) = \int_{-\pi/a}^{\pi/a}\frac{dk}{2\pi}\frac{e^{ik(x-z)}}{\zeta(k)+s}, \tag{B18}$$

where $\zeta(k) = (1-\cos k)$. In the continuum limit $a\to 0$, $(x-y) \propto a\sqrt{Dt/2} \propto a^2$, the above integral can be solved with the well-known result

$$\mathcal{L}P^z(x,s) = \frac{1}{\sqrt{4Ds}}e^{-\sqrt{s}|x-z|/\sqrt{D}}, \tag{B19}$$

which correspond to the solution of the diffusion equation for a one-dimensional Brownian motion with diffusion coefficient D—i.e.,

$$\frac{dP}{dt} = D\frac{d^2P}{dx^2}. \tag{B20}$$

Let us now compute all the functions needed to get G_4. First,

$$N(t) = \sum_{z\neq x}P^z_x(t) = \sum_{z\neq x}\mathcal{L}^{-1}\left(\frac{1}{s}\frac{\mathcal{L}P^z(x,s)}{\mathcal{L}P^x(x,s)}\right)(t),$$

where we used Eq. (B4). When $t \gg 1$ we get

$$N(t) = 4\frac{\sqrt{Dt}}{\sqrt{\pi}}.$$

Second, using the expression (B14) of G in terms of $\mathcal{L}P^z(x,s)$ we get

$$\mathcal{L}G(s,x-y) = 2\frac{\sqrt{D}}{s^{3/2}}\frac{e^{-\sqrt{s}|x-y|/\sqrt{D}}}{e^{-\sqrt{s}|x-y|/\sqrt{D}}+1}.$$

Changing variable in the inverse Laplace transform we get

$$G(t) = 4\sqrt{Dt}f\left(\frac{|x-y|}{\sqrt{2Dt}}\right),$$

where $f((|x-y|)/\sqrt{2Dt})$ equals

$$f\left(\frac{|x-y|}{\sqrt{2Dt}}\right) = \int_{-i\infty-\gamma}^{+i\infty-\gamma}\frac{e^{-\sqrt{2s}|x-z|/\sqrt{D}t}}{e^{-\sqrt{2s}|x-z|/\sqrt{D}t}+1}e^{-s}\frac{ds}{s^{3/2}}.$$

Finally $P_x^y(t)$ can be computed easily but it is always much smaller than the other terms in the exponential, so we are going to neglect it. The resulting expression for G_4 is

$$G_4(x-y,t) = \exp\left(-2\rho_v - \frac{8\rho_v}{\sqrt{\pi}}\sqrt{Dt}\right) \times\left\{\exp\left[\rho_v 2\sqrt{Dt}f\left(\frac{|x-y|}{\sqrt{2Dt}}\right)\right]-1\right\}. \quad \text{(B21)}$$

Note that the typical time scale is $\tau = 1/\rho_v^2 D$, and since we focus on $\rho_v \to 0$, we can rewrite the above expression as

$$G_4(x-y,t) = \exp\left(-\frac{\sqrt{8}}{\sqrt{\pi}}\sqrt{t/\tau}\right) \times\left\{\exp\left[2\sqrt{t/\tau}f\left(\rho_v\frac{|x-y|}{\sqrt{2t/\tau}}\right)\right]-1\right\}. \quad \text{(B22)}$$

Integrating over $x-y$ to get the χ_4 we find

$$\chi_4(t) = \frac{2}{\rho_v}\exp\left(-\frac{8}{\sqrt{\pi}}\sqrt{t/\tau}\right)\sqrt{2t/\tau}\int_0^{+\infty}dx\{\exp[2\sqrt{t/\tau}f(x)]-1\}. \quad \text{(B23)}$$

In particular when $t/\tau \ll 1$ we have

$$\chi_4(t) \propto \frac{1}{\rho_v}(t/\tau). \quad \text{(B24)}$$

The interpretation of this result is that at short times the defects do not intersect and the χ_4 is just the square of the number of average sites visited by a random walk until time t. We will see that this interpretation is indeed correct in any dimension.

Finally, after some algebra it is possible to obtain from Eq. (B24) that $\chi_4(t) \simeq (c/\rho_v)\exp[(-4/\sqrt{\pi})\sqrt{t/\tau}]$ at very large times (c is a numerical constant). Thus, as found in simulations, the normalized χ_4 does not go to zero as it happens in three dimensions.

2. Three dimensions and higher

Consider a symmetric random walk on a cubic lattice. The general expression for $P^z(x,s)$ is

$$P^z(x,s) = \int_{BZ}\frac{d^dk}{(2\pi)^d}\frac{e^{ik(x-z)}}{\zeta(k)+s}, \quad \text{(B25)}$$

where BZ means Brillouin zone and $\zeta(k) = \Sigma_{i=1}^d(1-\cos k_i)$ for a hypercubic lattice (k_i is the component of $\vec{k}$ in the direction i). Also in this case we consider the continuum limit $(x-y)/\sqrt{Dt/2} \propto O(1)$ and look for times t much larger than 1.

Let us again compute all the needed quantities: first, $N(t)$. In this case for $t \gg 1$ we find that

$$N(t) = D\left(\int_{BZ}\frac{d^dk}{\pi\zeta(k)}\right)^{-1}\mathcal{L}^{-1}\frac{1}{s^2}.$$

Hence $N(t) = c_1 tD$ where $c_1 = [\int_{BZ}d^dk/\pi\zeta(k)]^{-1}$.

Again, we neglect the $P_x^y(t)$ term and we focus on G in the continuum limit, for $t \gg a$. We get

$$\mathcal{L}G = \frac{1}{s^2}\frac{\int_{BZ}\frac{d^dk}{(2\pi)^d}\frac{e^{ik(x-z)}}{Dk^2+s}}{\left(\int_{BZ}\frac{d^dk}{(2\pi)^d}\frac{1}{Dk^2}\right)^2}.$$

Changing variable in the inverse laplace transform we get

$$G(t) = D^2\int_{-i\infty-\gamma}^{+i\infty-\gamma}e^{ts}\int_{BZ}\frac{d^dk}{(2\pi)^d}\frac{e^{ik(x-z)}}{Dk^2+s}\frac{\exp(ts)}{C^2s^2}ds.$$

Since we know the inverse laplace transform of the function resulting from the integral over k [it is simply $P^y(x,t)$] and each $1/s$ adds an integral, we finally get

$$G(t) = c_2(Dt)^2\int_0^1 du\int_0^u dv\frac{e^{-(x-y)^2/2Dtv}}{(2\pi Dtv)^{d/2}},$$

where c_2 is a numerical constant of order unity. From this expression, we finally obtain

$$G_4(x-y,t) = \exp(-2\rho_v - 2\rho_v c_1 Dt)\left[\exp\left(\rho_v(c_2Dt)^2 \times\int_0^1 du\int_0^u dv\frac{e^{-(x-y)^2/2Dtv}}{(2\pi Dtv)^{3/2}}\right)-1\right] \quad \text{(B26)}$$

and the results quoted in the main text.

3. Two dimensions

In two dimensions things are a bit tricky because of logarithmic corrections. Briefly, we obtain that

$$G_4(x-y,t) = \exp\left(-2\frac{c_3t}{\tau\ln t}\right)\frac{1}{\rho_v}c_4^2(t/\tau)^2\frac{1}{(\ln tD)^2}\int_0^1 du \times\int_0^u dv\frac{e^{-(x-y)^2/2Dvt}}{(2\pi Dvt)}, \quad \text{(B27)}$$

with c_3 and c_4 constants of order unity. Hence, integrating over $x-y$, we get

$$\chi_4(t) = \exp\left(-2\frac{c_3t}{\tau\ln t}\right)\frac{1}{2\rho_v}c_4^2(t/\tau)^2\frac{1}{(\ln tD)^2}. \quad \text{(B28)}$$

In particular when $t/\tau \ll 1$ we have

$$\chi_4(t) \propto \frac{1}{\rho_v}\left(\frac{t}{\tau \ln t}\right)^2. \tag{B29}$$

Again, since the number of sites visited on average by a RW in two dimensions goes like $t/\ln t$, at short times χ_4 is the square of the number of average sites visited until time t.

4. Density-density correlations

We now sketch the calculation for the density four point correlation, defined as

$$G_4^d(x-y,t) \equiv \langle [\eta_x(t)\eta_x(0)-\rho^2][\eta_y(t)\eta_y(0)-\rho^2]\rangle - \langle \eta_x(t)\eta_x(0)\rangle_c^2, \tag{B30}$$

with $\eta_x(t)=0,1$ if the site x is empty or occupied at time t, respectively. We start from

$$\langle \eta_x(t)\eta_x(0)\rangle_c^2 = \left(\left[\frac{1}{V}\sum_{z,z\neq x}[1-P^z(x,t)]\right]^{N_v} - \rho^2\right)^2.$$

Using that $\Sigma_z P^z(x,t)=1$ we get

$$\langle \eta_x(t)\eta_x(0)\rangle_c^2 = \exp(-4\rho_v)\{\exp[\rho_v P^x(x,t)]-1\}^2. \tag{B31}$$

In the limit $\rho_v \to 0$ we have

$$\langle \eta_x(t)\eta_x(0)\rangle_c^2 = [\rho_v P^x(x,t)]^2. \tag{B32}$$

Similarly we find that

$$\langle \eta_x(t)\eta_x(0)\eta_y(t)\eta_y(0)\rangle = \left(\frac{1}{V}\sum_{z,z\neq x,y}[1-P^z(x,t)-P^z(y,t)]\right)^{N_v} = \exp[-4\rho_v + 2\rho_v P^x(x,t) + 2\rho_v P^y(x,t)].$$

Collecting all the pieces together we finally get, at leading order in ρ_v,

$$G_4^d(x-y,t) = 2\rho_v P^y(x,t) \tag{B33}$$

for $x \neq y$. The interpretation of this equation is that the dynamical correlation between x and y is due to the fact that the *same vacancy* was in x at time 0 and t at time t or vice versa. Integrating over $x-y$ one finds that at long times $\chi_4(t) \propto 1/t^{d/2}$, showing no interesting structure.

[1] G. Adam and J. H. Gibbs, J. Chem. Phys. **43**, 139 (1965).
[2] See, e.g., M. D. Ediger, Annu. Rev. Phys. Chem. **51**, 99 (2000).
[3] E. Weeks, J. C. Crocker, A. C. Levitt, A. Schofield, and D. A. Weitz, Science **287**, 627 (2000).
[4] R. Richert, J. Phys.: Condens. Matter **14**, R703 (2002).
[5] E. Vidal-Russell and N. E. Israeloff, Nature (London) **408**, 695 (2000).
[6] L. A. Deschenes and D. A. Vanden Bout, Science **292**, 255 (2001).
[7] M. M. Hurley and P. Harrowell, Phys. Rev. E **52**, 1694 (1995) and references therein.
[8] A. Widmer-Cooper, P. Harrowell, and H. Fynewever, Phys. Rev. Lett. **93**, 135701 (2004).
[9] R. Yamamoto and A. Onuki, Phys. Rev. Lett. **81**, 4915 (1998) and references therein.
[10] G. Parisi, J. Phys. Chem. B **103**, 4128 (1999).
[11] B. Doliwa and A. Heuer, Phys. Rev. E **61**, 6898 (2000).
[12] C. Bennemann, C. Donati, J. Baschnagel, and S. C. Glotzer, Nature (London) **399**, 246 (1999); S. C. Glotzer, V. V. Novikov, and T. B. Schrøder, J. Chem. Phys. **112**, 509 (2000).
[13] N. Lacevic, F. W. Starr, T. B. Schrøder, V. N. Novikov, and S. C. Glotzer, Phys. Rev. E **66**, 030101(R) (2002); N. Lacevic and S. C. Glotzer, J. Phys.: Condens. Matter **15**, S2437 (2003); N. Lacevic, F. W. Starr, T. B. Schrøder, and S. C. Glotzer, J. Chem. Phys. **119**, 7372 (2003).
[14] Y. Hiwatari and T. Muranaka, J. Non-Cryst. Solids **235–237**, 19 (1998).
[15] F. Ritort and P. Sollich, Adv. Phys. **52**, 219 (2003).
[16] J. Jäckle and S. Eisinger, Z. Phys. B: Condens. Matter **84**, 115 (1991).
[17] P. Sollich and M. R. Evans, Phys. Rev. Lett. **83**, 3238 (1999).
[18] L. Berthier and J. P. Garrahan, J. Phys. Chem. B **109**, 3578 (2005).
[19] G. H. Fredrickson and H. C. Andersen, Phys. Rev. Lett. **53**, 1244 (1984); J. Chem. Phys. **83**, 958 (1984).
[20] J. P. Garrahan and D. Chandler, Phys. Rev. Lett. **89**, 035704 (2002); Proc. Natl. Acad. Sci. U.S.A. **100**, 9710 (2003).
[21] S. Whitelam, L. Berthier, and J. P. Garrahan, Phys. Rev. Lett. **92**, 185705 (2004).
[22] S. Whitelam, L. Berthier, and J. P. Garrahan, Phys. Rev. E **71**, 026128 (2005).
[23] L. Berthier and J. P. Garrahan, J. Chem. Phys. **119**, 4367 (2003); Phys. Rev. E **68**, 041201 (2003).
[24] W. Kob and H. C. Andersen, Phys. Rev. E **48**, 4364 (1993).
[25] C. Toninelli, G. Biroli, and D. S. Fisher, Phys. Rev. Lett. **92**, 185504 (2004); J. Stat. Phys. (to be published).
[26] S. H. Glarum, J. Chem. Phys. **33**, 1371 (1960).
[27] A. Pan, D. Chandler, and J. P. Garrahan, e-print cond-mat/0410525.
[28] S. Franz and G. Parisi, J. Phys.: Condens. Matter **12**, 6335 (2000); C. Donati, S. Franz, G. Parisi, and S. C. Glotzer, J. Non-Cryst. Solids **307**, 215 (2002).
[29] T. R. Kirkpatrick and D. Thirumalai, Phys. Rev. A **37**, 4439 (1988).
[30] L. Berthier, Phys. Rev. E **69**, 020201(R) (2004).
[31] P. Mayer, H. Bissig, L. Berthier, L. Cipelletti, J. P. Garrahan, P. Sollich, and V. Trappe, Phys. Rev. Lett. **93**, 115701 (2004).
[32] G. Biroli and J.-P. Bouchaud, Europhys. Lett. **67**, 21 (2004).
[33] L. Berthier, Phys. Rev. Lett. **91**, 055701 (2003).
[34] T. Kirkpatrick and P. Wolynes, Phys. Rev. B **36**, 8552 (1987); T. R. Kirkpatrick, D. Thirumalai, and P. G. Wolynes, Phys. Rev. A **40**, 1045 (1989).
[35] J.-P. Bouchaud and G. Biroli, J. Chem. Phys. **121**, 7347

(2004).
[36] G. Tarjus and D. Kivelson, J. Chem. Phys. **103**, 3071 (1995); D. Kivelson and G. Tarjus, Philos. Mag. B **77**, 245 (1998).
[37] W. Götze and L. Sjögren, Rep. Prog. Phys. **55**, 241 (1992); W. Götze, Condens. Matter Phys. **1**, 873 (1998); W. Kob, in *Slow Relaxations and Non-equilibrium Dynamics in Condensed Matter*, edited by J.-L. Barrat, M. Feigelman, J. Kurchan, and J. Dalibard (Springer, Berlin, 2003).
[38] T. S. Grigera, A. Cavagna, I. Giardina, and G. Parisi, Phys. Rev. Lett. **88**, 055502 (2002).
[39] A. Montanari and G. Semerjian, e-print cond-mat/0412023.
[40] M. Vogel, B. Doliwa, A. Heuer, and S. C. Glotzer, J. Chem. Phys. **120**, 4404 (2004).
[41] L. V. Woodcock, C. A. Angell, and P. Cheeseman, J. Chem. Phys. **65**, 1565 (1976).
[42] S. A. Brawer, Phys. Rev. Lett. **46**, 778 (1981); J. Chem. Phys. **75**, 3516 (1981); D. A. Litton and S. H. Garofalini, J. Non-Cryst. Solids **217**, 250 (1997).
[43] See, e.g., C. Masciovecchio, G. Ruocco, F. Sette, M. Krisch, R. Verbeni, U. Bergmann, and M. Soltwisch, Phys. Rev. Lett. **76**, 3356 (1996).
[44] Note, however, that in a numerical simulation with a box of size, say, $L=10a$, the elastic contribution will saturate after a time $L/V\sim 1$ ps. This contribution will therefore be hard to see unless much larger sizes can be simulated.
[45] G. Biroli, L. Berthier, and J.-P. Bouchaud (unpublished).
[46] D. S. Fisher and D. A. Huse, Phys. Rev. B **38**, 373 (1988).
[47] S. Redner, *A Guide to First Passages Processes* (Cambridge University Press, Cambridge, U.K., 2001).
[48] *Fluctuation Phenomena Studies in Statistical Mechanics*, Vol. 7 of edited by E. W. Montroll and J. L. Lebowitz (North-Holland, Amsterdam, 1979).
[49] E. Bertin, J. P. Bouchaud, and F. Lequeux, e-print cond-mat/0501192.
[50] J.-P. Bouchaud, in *Slow Relaxations and Non-equilibrium Dynamics in Condensed Matter*, edited by J.-L. Barrat, M. Feigelman, J. Kurchan, and J. Dalibard (Springer, Berlin, 2003).
[51] M. B. Isichenko, Rev. Mod. Phys. **64**, 961 (1992).
[52] L. Berthier, D. Chandler, and J. P. Garrahan, Europhys. Lett. **69**, 320 (2005).
[53] W. Kob and H. C. Andersen, Phys. Rev. Lett. **73**, 1376 (1994).
[54] M. Nauroth and W. Kob, Phys. Rev. E **55**, 657 (1997).
[55] J.-L. Barrat and A. Latz, J. Phys.: Condens. Matter **2**, 4289 (1990).
[56] D. R. Reichman and R. A. Denny (unpublished).
[57] G. Tarjus, D. Kivelson, and P. Viot, J. Phys.: Condens. Matter **12**, 6497 (2000).
[58] G. Marty and O. Dauchot, Phys. Rev. Lett. **94**, 015701 (2005).
[59] H. Castillo, C. Chamon, L. F. Cugliandolo, J. L. Iguain, and M. P. Kennett, Phys. Rev. B **68**, 134442 (2003); C. Chamon, P. Charbonneau, L. F. Cugliandolo, D. R. Reichman, and M. Sellitto, J. Chem. Phys. **121**, 10120 (2004).
[60] A. Lefèvre, L. Berthier, and R. Stinchcombe, e-print cond-mat/0410741.
[61] J. P. Bouchaud and G. Biroli, e-print cond-mat/0501668.
[62] R. Arratia, Z. Ann. Prob. **11**, 382 (1983).